

Metal–Organic Frameworks (MOFs) and Their Composites for Oil/Water Separation

Abdullah M. Abudayyeh,[∇] Lila A.M. Mahmoud,[∇] Valeska P. Ting, and Sanjit Nayak*

Cite This: *ACS Omega* 2024, 9, 47374–47394

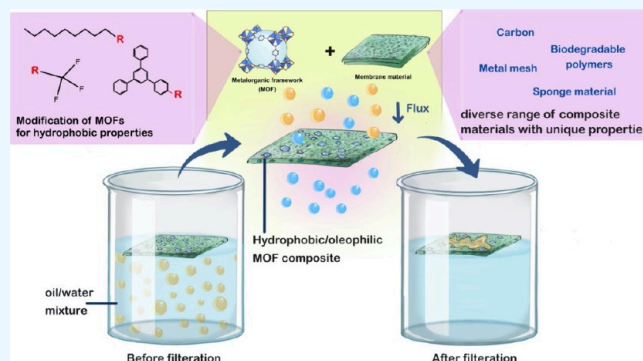
Read Online

ACCESS |

Metrics & More

Article Recommendations

ABSTRACT: Contamination of water by oil-based pollutants is a major environmental problem because of its harmful impact on human life, marine life, and the environment. As a result, a wide range of materials are being investigated for the effective separation of oil from water. Among these materials, metal–organic frameworks (MOFs) and their composites have emerged as excellent candidates due to their ultraporous structures with high surface areas that can be engineered to achieve high selectivity for one of the phases in an oil/water mixture for efficient water filtration. However, the often nanocrystalline/microcrystalline form of MOFs combined with challenges of processability and poor stability in water has largely limited their use in industrial and environmental applications. Hence, considerable efforts have recently been made to improve the performance and stability of MOFs by introducing hydrophobic functional groups into the organic linkers and fabricating polymer-MOF composites to increase their stability and recyclability. In addition, the use of biobased or biodegradable MOF composites can be particularly useful for applications in natural environments. This Review presents recent advances in the field of hydrophobic MOFs and MOF-based composites studied for the separation of oil from oil/water mixtures, with an account of future challenges in this area.



1. INTRODUCTION

Water pollution involves the contamination of natural bodies of water such as oceans, lakes, and groundwater with harmful chemicals that are not only detrimental to human health but also have a significant impact on wider environment and ecosystem. Hydrocarbon contamination has been identified as one of the main contributors to water pollution, which can result from food waste, sewage, and industrial effluents. In the mining industry, a standard mining operation can produce up to 140 000 L of oil-contaminated wastewater per day.¹ Leaking oil pipelines and fracking operations have also been reported to contaminate ground and surface water.² In addition, oil spills from tankers can deposit huge quantities of oil contaminants into the oceans. For example, more than ~342 000 t of crude oil were spilled into European water in two catastrophic oil spills, namely, the Torrey Canyon in Cornwall (England, 1967) and the Amoco Cadiz in Brittany (France, 1978).³ These accidents caused significant damage to ecological systems and marine life, not to mention the depletion of resources and laborious efforts required to eliminate the toxic organic chemicals and other types of pollutants released during the spill. Although strict measures and regulations have been put in place for the transportation of oil, oil spill incidents have increased over the last couple of decades. Investigations into the effect of oil spill contamination on human health suggest a

correlation with acute physical, psychological, genotoxic, and endocrine effects.⁴ Consequently, the purification of water from oil residues is a key area of research. Considerable efforts have been made to develop effective and inexpensive materials for water treatment.⁵ Regulations have been imposed by societies and governments to ensure clean water seawater and wastewater through rigorous treatment. Current techniques for oil/water separation to mitigate oil contamination are mainly based on physical treatment methods, which include gravity-assisted separation, centrifugation, filtration, and flotation. Other methods based on electrochemical or biological treatments are also occasionally used. In general, most industrial oil/water separation methods are laborious, energy and capital intensive, and often inefficient due to a low selectivity for oil over water.⁶

Besides the above methods, material-based approaches have also been investigated for oil/water separation. A wide range of

Received: August 28, 2024
Revised: November 1, 2024
Accepted: November 7, 2024
Published: November 19, 2024



materials have been developed and tested for oil/water separation over the last two decades. These include porous carbon-based materials, sponge-based materials, fibrous materials based on biomass,^{7,8} and polymer materials,⁹ as well as extensive work on nanomaterials for oil separation, which can be found elsewhere.^{10–12} The surface of a material to be used in oil/water separation needs to be tuned in such a way as to repel water by having nonpolar components (hydrophobic, or “water-hating”) while bearing high affinity to absorb (for bulk material) or adsorb (for filter materials) oil (oleophilic or superoleophilic, “oil-loving”) to allow the separation of oil from oil/water mixtures.¹¹ Materials with opposite affinities can also be used. For example, materials for water removal from oil/water mixtures could have highly polar surfaces, so they display hydrophilic (water-loving) and superoleophobic (oil-hating) characters.¹³ It is widely believed that both the surface topography and the chemical composition of a material determine its superhydrophobicity/superoleophilicity.¹⁴ Based on that, approaches for tuning the surface of a material intended for oil/water separation either by chemical modification or by assimilation within composites in combination with matrix materials such as sponges, clays, polymers, foams, or carbon materials have recently attracted much interest.¹⁵ Nevertheless, there is a need to circumvent the fact that some composite materials have a high tendency to absorb water on their own, which seriously limits their performance in oil/water separation.

Metal–organic frameworks (MOFs) are a class of three-dimensional coordination polymers connecting metal clusters (nodes) and organic linkers (struts) through strong coordination bonds, often forming permanent voids.¹⁶ Due to their high porosity and high surface area along with possible incorporation and opportunity for surface modification by desired functionalities, MOFs have been the subject of great interest for their potential applications in various fields,¹⁶ like gas storage,¹⁷ separation,¹⁸ catalysis,¹⁹ sensing,²⁰ heavy metal removal from water,²¹ herbicides,^{22,23} and drug delivery.^{24–26} Owing to a handy ability to incorporate a diverse range of chemical compositions, thousands of MOFs have been synthesized so far. Among them, more than 100 hydrophobic MOFs,²⁷ in addition to their composites, have been synthesized and studied for water treatment and water/oil separation.^{6,28,27,29}

It may also be the case that when some rationally designed hydrophobic MOFs are incorporated into highly water repellent surfaces, such as activated resins or fluorinated graphene, the resulting MOF-based composite can have much better hydrophobic behavior,^{13,30} leading to better separation performance for oil/water mixtures.

Due to the poor hydrolytic stability,³¹ and the typically nanocrystalline or powder forms of many MOFs, with no “free standing ability”, direct application of MOFs in oil/water separation might be limited to dispersion, which may result in poor recoverability and recyclability and insufficient absorption capacity in some cases. Building upon that, two main strategies to improve oil/water separation by MOF-based materials have been reported in the literature: the first is post-synthetic modification of the surface of MOFs to improve their hydrophobic/oleophilic properties, and the second is embedding hydrophobic MOFs into other supporting materials to form composites or membranes, for example, by incorporating MOFs into a polymer matrix,³¹ fibers, or sponges³² or through the intercalation of MOFs within porous networks.³⁰

The following sections will provide an up-to-date account of the advances in hydrophobic MOFs and their composites used for the separation of oil/water mixtures. In the first part, approaches used to synthesize hydrophobic MOFs are briefly discussed, followed by an overview of the metrics used to assess the performance of the MOF composites for oil/water separation. In the following part, the difference in performance between as-prepared hydrophobic MOFs and their composites is critically discussed. Additionally, attempts to synthesize Bio-MOFs and biodegradable MOF composites and their potential application in oil/water separation are also highlighted. Finally, the challenges in this important field of study are outlined, with potential directions for future development.

2. EXPERIMENTAL TECHNIQUES FOR EVALUATION OF WATER/OIL SEPARATION

There are some quantitative and qualitative experimental tests to assess the efficiency of materials for water/oil separation. These include tests of hydrophobicity, such as water contact angle (WCA) and absorption capacity measurements, recyclability, and competitive water–hydrocarbon (usually toluene) adsorption experiments. The water content of the MOF composite can also be indicated by IR spectroscopy via monitoring bands originating from OH stretching and H–O–H bending at 3400 and 1621 cm^{-1} , respectively. Thermogravimetric (TG) measurement provides not only a quantitative analysis of the amount of water adsorbed by the MOFs/MOF composites but also the stability of the framework during MOF–water interaction within a broad temperature range.²⁹ A number of parameters are used to evaluate the performance of MOF composites for the removal of oil from oil/water mixtures, such as water contact angle, absorption capacity, separation flux, separation efficiency, and durability. These parameters will be discussed in more detail in the following sections. The formulas used in the following sections are based on normal pressure, where liquid flow is caused by gravity and no external pressure is used.

2.1. Water Contact Angle. The hydrophobic behavior of MOFs and their composites is usually indicated by the water contact angle (WCA) measurement. MOF composites with WCA angles greater than 90° (Figure 1, left) suggest that the

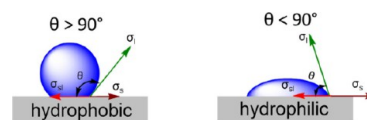


Figure 1. Water contact angle of (left) a hydrophobic surface ($\theta < 90^\circ$) and (right) a hydrophilic surface $\theta > 90^\circ$. Figure was adopted and modified based on ref 27.

surface repels water and has low wettability. In such instances, the MOF composite is regarded as hydrophobic. In contrast, if the surface has affinity to water, the WCA will be less than 90° (Figure 1, right) and the MOF composite is considered as hydrophilic. Rarely, but of great interest, when the MOF or its composite has a contact angle with water greater than 150° , the material is considered as superhydrophobic.

The contact angle of a water drop (θ) on a surface can be calculated using Young's equation (eq 1).

$$\sigma_l \times \cos \theta = \sigma_s - \sigma_{sl} \quad (1)$$

Table 1. Summary of Hydrophobic MOFs/Composites with Their Hydrophobic Properties, Water Contact Angle (WCA), and Applications in Oil/Water Separation^a

MOF/MOF composite	SBU/composite	modification / hydrophobic ability?	MOF composite Synthesis method	WCA / ° At pH 7	absorption Capacity	Flux / L m ⁻² h ⁻¹	Water/Oil	Reusability/cycles	Ref, Year
UHMOF-100	4,4'-[[3,5-bis(trifluoromethyl)phenyl]azanediyl]dibenzoic acid	CF ₃ moiety	-	177°	-	-	toluene, hexadecane, chloroform, biodiesel and crude oil	3	⁵² (2016)
UHMOF-100/PDMS/PP	UHMOF-100 on polypropylene support	MOF composite	Spray coating of MOF and PDMS on a PP fabric support	135°	40–70	85		10	
S-MIL-101 (Cr)	Cr ₃ O(OH)(HO) ₂ -(bdc)	-	-	-	118–281	-	CH ₂ Cl ₂ , hexane, toluene petroleum ether	-	⁶¹ (2019)
S-MIL-101 (Cr)/Octadecylamine	Cr ₃ O(OH)(HO) ₂ -(bdc)-NH ₂	Octadecylamine alkyl chain	stirring the activated MOFs in a 10 mM octadecylamine toluene solution at 120 °C for 24 h	156°	142–369	-		10	
UiO-66-NH-C18	Zr ₆ O ₈ bdc-NH ₂	C18 Alkyl chain	Postsynthetic modification: coordinating to metal center	151.6°	-	-	Decane Toluene DMF Acetone Ethyl acetate diesel n-hexane dichloromethane	3	³² (2020)
UiO-66-NHC18@sponge	Zr ₆ O ₈ bdc-NH ₂ / melamine formaldehyde sponge		Postsynthetic modification: Amidation reaction	141°	32.3–66.1	-		10	
UPC-21	Cu ₂ (COO) ₄ pentiptycene	Poly aromatic hydrophobic linker	-	145°	-	-	Toluene Hexane gasoline naphtha, crude oil	-	⁴¹ (2017)
UPC-29	Cu ₂ (COO) ₄ pentiptycene	Poly aromatic hydrophobic linker	-	178°	-	-	Naphtha Gasoline diesel	-	⁴² (2019)
pristine ZIF-8	Zn-melM=2-methylimidazole	-	-	56°	10–150	-	-	-	³⁰ (2016)
HFGO@ZIF-8	Zn-melM=2-methylimidazole / Highly Fluorinated graphene oxide	fluorinated graphene oxide layers	addition of a mixture of exfoliated HFGO sheets in chloroform during the formation of ZIF-8 nanocrystals at the liquid–solid interface in methanolic medium	162°	20–280	-	Vegetable oil Dodecane Octane Heptane Hexane Pentane benzene toluene DMF	4	
Sponge@HFGO@ZIF-8	Zn-melM=2-methylimidazole/ Highly Fluorinated graphene oxide /commercial sponge								
			immersing a commercial sponge into the reaction mixture of exfoliated HFGO and a methanolic solution of the ZIF-8 growth components and letting it sit in solution Overnight		150–600		Veg oil Dodecane Silicon oil Coconut oil Petroleum ether chloroform		

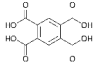
Table 1. continued

MOF/MOF composite	SBU/composite	modification / hydrophobic ability?	MOF composite Synthesis method	WCA / ° At pH 7	absorption Capacity	Flux / L m ⁻² h ⁻¹ ,	Water/Oil	Reusability/cycles	Ref, Year
SHMOF, [Hf ₆ O ₄ (OH) ₄ (TFND C) ₆] 6H ₂ O·2DMF	Hf ₆ O ₄ (OH) ₄ TFNDC	CF ₃ group	-	131°	-	1300-1800	gasoline, DCM, CHCl ₃ , CCl ₄ , petrol, kerosene, crude oil, diesel, toluene, hexane, EtOAC	-	⁵⁰ (2022)
SHMOF-PP	SHMOF on polypropylene		In situ coating on polypropylene (PP) fabric	160°	29-39	1845-1899		20	
UiO-66'@CF3	Zr ₆ O ₈ bdc-COCF ₃	COCF ₃ group	Postsynthetic substitution of OH groups to OCCF ₃ groups	104°	-	-	gasoline, DCM, CHCl ₃ , CCl ₄ , motor oil, kerosene, toluene, hexane, EtOAC	30	⁶⁸ (2021)
UiO-66'@CF3@melamine	PDA-Polydopamine melamine sponge		a mixture of MOF and polymer was homogeneously coated on a small piece of PDA-coated sponge and it was fully dried at a temperature of 125 °C.	145°	27-37	1959, 1931, 1957 and 2028 for water/CHCl ₃ , water/kerosene, and water/gasoline, respectively			
PC-MIL-100	MOF derived carbon	porous carbon calcination at 1073 K	-	-	-	-	gasoline, DCM, CHCl ₃ , silicone, hexadecane, dodecane, heptane	-	⁷² (2020)
MFS-PC-MIL-100(Fe)	melamine formaldehyde sponge		dispersion method	145°	10-18 g/g			10	
A-MOF {[Eu(HBDO)-(CH ₂ OH)(H ₂ O) ₂]}(H ₂ O) _{0.5} } _n	[Eu ₂ (COO) ₂] H4bdo = 2,5-bis(3,5-dicarboxylphenyl)-1,3,4-oxadiazole	post-synthetic modification by alkylamine chains	-	142°	4517-14728 wt %	-	Cyclohexane, toluene, n-hexane, gasoline, n-heptane, hexadecane, silicone oil, chloroform, tetrachloromethane, dibromoethane	50	⁵¹ (2020)
A-MOF-rGA superhydrophobic aerogel AM-rGA	Amylamine modified MOF on reduced graphene oxide (rGO)		A-MOF was mixed with rGO and assembled as hydrogel using one pot method then formed through freeze drying process	132°					
NH ₂ -UiO-66(Zr)-shp	2-aminoterephthalic acid	Post synthetic MOF modification by adding phenylsilane (PhSiH ₃) on metal oxo sites	-	161°	-	-	toluene	-	⁶⁰ (2019)
UiO-66-F	2-aminoterephthalic acid	Post synthetic modification by fluorination	-	145°	163-351 wt%	-	EtOH, MeOH, CHCl ₃ , and toluene	10	⁷⁹ (2021)
2D pillard MOF nanosheets [Cd ₃ (IDC) ₂ (HIDC)(bpy) ₂ ·(H ₂ O) ₃]·2NO ₃ ·2H ₂ O } _n And [Cd ₃ (IDC) ₂ (bpy) ₂ ·(H ₂ O) ₂]·NO ₃ ·3.5H ₂ O } _n	IDC HIDC bpy py	Ligand replacement To form 2D nanosheets from 3D microcrystals	-	129° and 139°, respectively	-	-	Cyclohexane 1,2-dichloroethane	-	⁸⁰ (2019)
MOF-5@FMWCNTs	BDC linker MOF on functionalized multiwalled carbon nanotubes	Composite of MOF-5 and carboxy functionalized carbon nanotubes	Microwave assisted synthesis of MOF-5 in a solution containing FMWCNT	-	-	-	-	-	⁸¹ (2018)
PESD-1>Guest	H ₃ BTMB	-	-	-	-	-	-	-	⁵⁴ (2014)

Table 1. continued

MOF/MOF composite	SBU/composite	modification / hydrophobic ability?	MOF composite Synthesis method	WCA / ° At pH 7	absorption Capacity	Flux / L m ⁻² h ⁻¹ ,	Water/Oil	Reusability/cycles	Ref, Year
F-ZIF-90@PDA-MF	Imidazolate linker PDA MF	Flourinated composite of PDA, MF and ZIF-90	PDA-assisted growth of ZIF-90 on a MF sponge.	153°	9.4–130.4 g g ⁻¹	up to 7.1×10 ⁵ L m ⁻² h ⁻¹		20	⁸² (2023)
SnTCPP-PTS SnTCPP-SQL SnTCPP-SHE	TCPP: tetrakis(4-carboxylphenyl)porphyrin	-	-	170° 82° 165°	-	-	-	3	⁵³ (2022)
ZIF-8 coated mesh	Zn-melM: 2-methylimidazole	ZIF-8 Stainless steel mesh composite	ZIF-8 coated stainless steel mesh via simple secondary growth method	OCA: 80°	-	10.2×10 ⁴	Diesel Soybean oil Cyclohexane Pump oil	10	⁸³ (2021)
Bio-MOFs									
Cu-Asp MOF TF@Cu-Asp-MOF	Cu aspartic acid	Cu-Asp MOF Was prepared by electrochemical method	A textile fabric was sprayed by previously prepared Cu-Asp MOF@SA solution, then rinsed with EtOH and dried at 60 °C for 2 hours	158°	85-160	-	n-hexane, petroleum ether and silicon oil	10	³³ (2022)
SH-UiO-66' UiO-66-NH-NHCO(CH ₂) ₄ CH ₃ SH-UiO-66@sponge	palmitamidoterephthalic acid (H ₂ BDC-NH-R, R: -NH-CO-(CH ₂) ₄ -CH ₃)	post-synthetic modification by alkylamine chains	MOF was added to crosslinked PDMS-PDMS polymer solution, mixed suspension was sonicated and heated at 40 °C for 1 h to cross-polymerize on melamine sponge composite	168° 169°	43.8 - 97.2	58 263–47 416	gasoline, DCM, CHCl ₃ , CCl ₄ , motor oil, kerosene, toluene, hexane, Diesel, Crude oil EtOAC	70	³⁹ (2023)
ZIF-8 ZIF-8/CA ZIF-8-doped cellulose acetate foam	Zn-melM=2-methylimidazole	-	thermally induced non-solvent induced phase separation (TINIPS) method CA was added to the ZIF-8 solution and stirred (1000 r/min) at 70 °C until completely dissolved.	153°	6.89–14.61	-	soybean oil, CCl ₄ xylene	6	⁸⁴ (2023)
ZIF-8@MF	Zn-melM=2-methylimidazole/	-	in situ growth method	145°	68–165	-	n-hexane, tetrachloroethylene, cyclohexane, trichloromethane, petroleum ether, 1,2-dichloroethane, methylbenzene	20	⁷¹ (2023)

Table 1. continued

MOF/MOF composite	SBU/composite	modification / hydrophobic ability?	MOF composite Synthesis method	WCA / ° At pH 7	absorption Capacity	Flux / L m ⁻² h ⁻¹ ,	Water/Oil	Reusability/cycles	Ref, Year
ZIF-8@PLA aerogel	Zn-melM=2-methylimidazole/	-	physical blending and thermally induced phase separation with the assistance of water see below: ZIF-8 was uniformly dispersed in deionised water and then dropped into a mixture of PLA and 1,4-dioxane under magnetic stirring. The mixture was heated at 60 °C and stirred for 1 h to obtain a uniform composite dispersion.	147°	15–30	13 000 – 35 000	heptane, carbon tetrachloride, pentane, n-hexane	20	⁶⁹ (2021)
ZIF-67@PLA aerogel	2-methamidazole	-	physical blending and thermally induced phase separation	132° for ZIF-67 107° for PLA	10-25	51180-71660	petroleum ether, carbon tetrachlorid, heptane, cyclohexane, isooctane.	20	⁷⁰ (2023)
C3N4/Cu-MOF@cotton	Cu(CH3COO)2 Btec : Pyromellitic acid 	simple hydrothermal method	simple ground soaking method, in which the cotton was soaked in the C3N4/Cu-MOF solution	150°	-	-	engine oil, n-hexane, castor oil, acetone, DCM, and canola oil	10	⁶⁵ (2023)

^ashp: superhydrophobic, BTFM: 2,5-bis(trifluoromethyl)terephthalic acid, DABCO: 1,4-diazabicyclo[2.2.2]octane, PDMS: polydimethylsiloxane, PP: polypropylene, HFGO: highly fluorinated graphene oxide, TFNDC = 1-(2,2,2-trifluoroacetamido)naphthalene-3,7-dicarboxylate, MFS: melamine formamide sponge, H₄bdo: 2,5-bis(3,5-dicarboxylphenyl)-1,3,4-oxadiazole, BTFM: 2,5-bis(trifluoromethyl)terephthalic acid, DABCO:1,4-diazabicyclo[2.2.2]octane, H3IDC: imidazole-4,5-dicarboxylic acid, bpy: 4,4'-bipyridine, py: pyridine, BDC: 1,4-benzenedicarboxylate, MWCNT: multi-walled carbon nanotubes, FMWCNT: functionalized multi-walled carbon nanotubes, MF: melamine formaldehyde.

In this equation, σ_1 represents the surface tension of water, θ is the contact angle between the water drop and the surface, σ_s is the surface free energy, and σ_{sl} is the interfacial tension between the surface and the water drop.^{27,29}

2.2. Absorption Capacity. Another parameter to assess the performance of a MOF composite for oil/water separation is its absorption capacity (k). It measures the ability of MOF composites to absorb oil, expressed as grams per gram of sample, by measuring the mass of the MOF composite sample before and after immersion in an oil/water mixture. Equation 2 is used to calculate the absorption capacity of different materials.³³

$$\text{Absorption capacity } (k) = \frac{W_{\text{wet}} - W_0}{W_0} \times 100\% \quad (2)$$

In this equation, the amount of oil absorbed by the MOF composite, which can be calculated by subtracting the mass of the MOF composite before absorption (W_0) from the mass of the MOF composite after absorption (W_{wet}), is compared to its initial mass (W_0). MOF composites reported to date have shown a wide range of absorption capacities between 5 and 600 wt % (Table 1).³⁰

2.3. Separation Flux. Separation flux reflects the amount (by volume) of a liquid mixture (V) passing through per unit of effective area (A) of a MOF composite per unit time (t).³³ Equation 3 below is used to calculate the separation flux of a MOF composite material during the separation of oil/water mixtures. High flux through a membrane and good retention of oil are crucial factors for membranes for oil/water separation technology.^{34,35} This means that an efficient membrane must allow a high amount of the oil/water mixture to be filtered through in a given period of time while maintaining high retention of oil. Flux is dependent on many factors, including

intrinsic factors of the membrane such as surface roughness, surface chemistry, pore size, and thickness.³⁶

$$\text{Separation flux} = \frac{V}{(A \times t)} \quad (3)$$

2.4. Separation Efficiency. Separation efficiency (R) is a measure of the membrane's ability to separate oil from an oil/water mixture. R is an important metric and can be used to measure the efficiency of a MOF or MOF composite for the separation of oil from an oil/water mixture. Equation 4 is usually used to calculate R .

$$\text{Separation efficiency } (R) = \left(1 - \frac{C_p}{C_o}\right) \times 100\% \quad (4)$$

Here, C_o is the initial oil concentration in the oil/water mixture and C_p is the final concentration of oil in the oil/water mixture after separation.³³ The separation efficiency depends on the wettability of the membrane, as it reflects the membrane's ability to separate the oil and water phases by their surface energy differences.³⁷ Degradation of the materials and other factors like fouling can eventually reduce the porosity of membranes and can negatively impact the separation efficiency of the material.

2.5. Durability and Recyclability. Durability of the MOF material used in oil separation can be defined as the ability to withstand harsh conditions without being chemically altered or physically damaged during separation. One way to test the durability of the MOF composite for oil separation from water is to determine the number of cycles that MOF composites can perform oil/water separation processes without significant degradation. Also of note, harsh conditions can have a great impact on the performance and hence the durability of the MOF composite; those include but are not limited to exposure

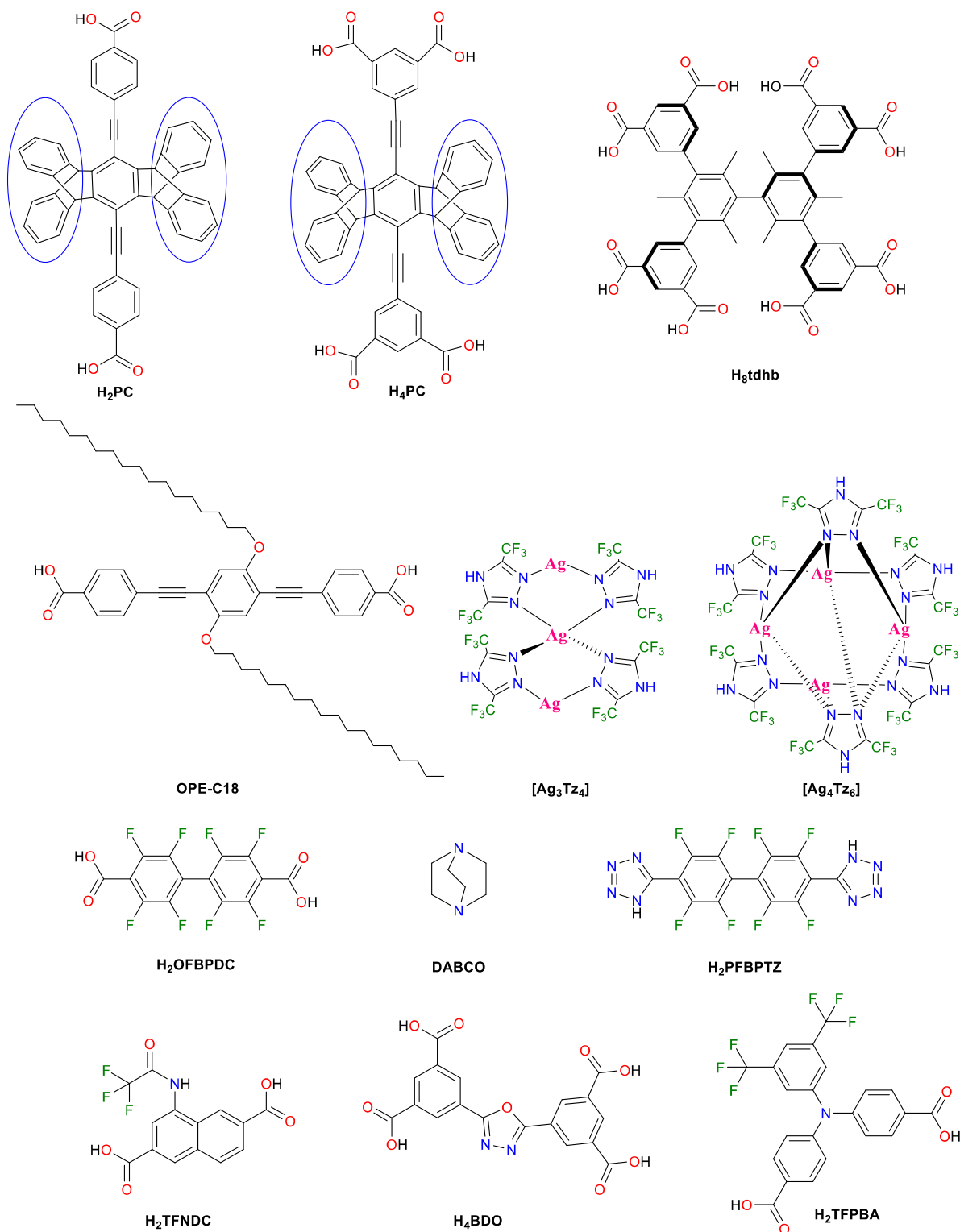


Figure 2. Selected building blocks used to synthesize hydrophobic MOFs. H₂PC (cyclopentiptycene dicarboxylic acid ligand),⁴⁰ H₄PC (cyclopentiptycene tetracarboxylic acid ligand),⁴⁶ H₈tdhb (3,3',5,5'-tetrakis(3,5-dicarboxyphenyl)-2,2',4,4',6,6'-hexamethylbiphenyl),⁴³ OPE-C18 (dialkoxyoctadecyl-oligo-*p*-phenyleneethynylene)dicarboxylate,⁴⁷ Tz (3,5-bis(trifluoromethyl)-1,2,4-triazolate),⁴⁸ H₂OFBPD (2,2',3,3',5,5',6,6'-octafluorobiphenyl-4,4'-dicarboxylic acid),⁴⁹ H₂TFNDC (1-(2,2,2-trifluoroacetamido)-naphthalene-3,7-dicarboxylic acid),⁵⁰ H₄BDO (2,5-bis(3,5-dicarboxylphenyl)-1,3,4-oxadiazole),⁵¹ and H₂TFPBA (4,4'-([3,5-bis(trifluoromethyl)phenyl]azanediyl)benzoic acid).⁵²

to high or low pH, variation in temperature and pressure, or any sort of mechanical forces that cause damage. Durability is highly dependent on the composition and mechanical properties of the material such as toughness, hardness, and

tensile strength. Many MOFs are prone to degradation at low or high pH, and sometimes they are incorporated within composite materials to improve their chemical and mechanical stability.

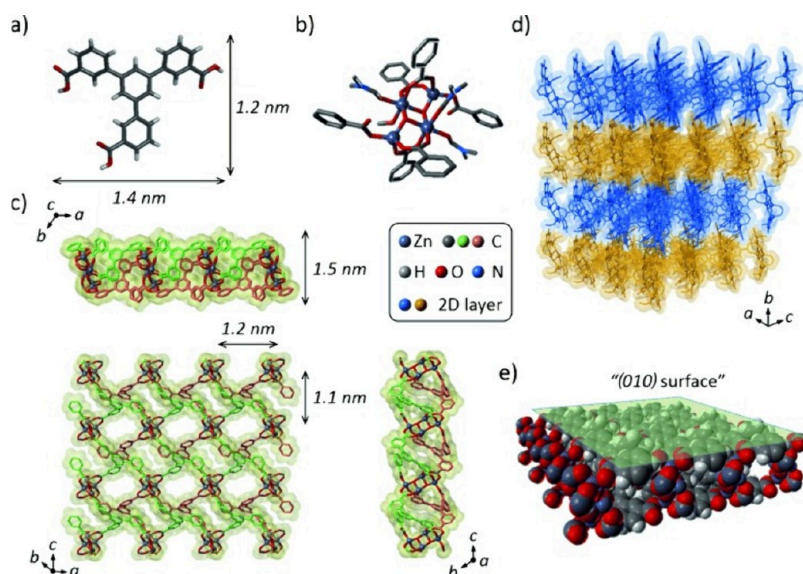


Figure 3. Molecular structures showing (a) the H₃BTMB linker and (b) the coordination mode of the PCP's [Zn₄(μ₃-OH)₂]⁶⁺ cluster. (c) 2D layer arrangement of the coordination polymer, (d) stacking of 2D layers to form 3D structures, and (e) the (0k0) surface with terminating phenyl moieties. Adapted with permission from ref 54.

The reported recyclability of the MOF composites used in oil/water separation ranges between 6 cycles for ZIF-8-doped cellulose acetate foam³⁸ and up to 70 cycles for a superhydrophobic melamine sponge composite (SH-UiO-66@ sponge) of a Zr-based MOF with a long-chain hydrocarbon-based linker.³⁹ Different approaches have been used to study the recyclability of the composites, including reuse upon simple gravity filtration through the membranes and continuous operation using peristaltic pumps.^{38,39}

3. HYDROPHOBIC MOFs FOR OIL/WATER SEPARATION

Hydrophobicity is often an indicator of the oleophilicity of a material; therefore, it gives an idea of the expected performance for oil/water separation. By definition, if the MOF material displays WCA > 90° (see Figure 1), then the MOF is considered hydrophobic; if the WCA ≥ 150°, then it suggests that the MOF has superhydrophobic character.²⁹ A number of parameters contribute toward the hydrophobicity of MOFs, including the presence of hydrophobic linkers or the attachment of hydrophobic groups on the linker or on coordinatively unsaturated metals by post-synthetic modification. Crystal engineering also plays an important role in aligning hydrophobic groups on the surface of the MOFs, enhancing hydrophobic properties of the MOFs. Each of these parameters is discussed in the following section.

3.1. Use of Hydrophobic Linkers. The hydrophobicity of the linkers can originate from several factors, including the presence of π-electron-rich aromatic groups, long alkyl chains, or fluorinated groups. The use of π-bond-rich hydrophobic linkers such as cyclopentacytene^{40–42} or aromatic linkers⁴³ is one of the primary strategies for the synthesis of hydrophobic MOFs. Pentipitycene is a type of ipitycene, which is a rigid organic ligand with multiple phenyl rings bonded to a bicyclooctatriene unit system. The rigidity of the phenyl-bicyclooctatriene head unit does not allow ipitycene ligands to pack efficiently in the solid state, resulting in inevitable void spaces being formed by the structure. Thus, ipitycene ligands have attracted much interest in material and supramolecular

chemistry.^{44,45} In 2015, MacLachlan et al. first reported a cyclopentipitycene dicarboxylic acid ligand, H₂PC (Figure 21), to synthesize a paddle-wheel zinc-based MOF (PMOF).⁴⁰ Subsequently, in 2017, Sun and co-workers demonstrated how using the cyclopentipitycene tetracarboxylic acid analogue,⁴⁶ H₄PC (Figure 2), can tune the hydrophobicity and water stability of a copper-based MOF, UPC-21, with excellent potential for application in oil/water separation.⁴¹ Following the same strategy, in 2019, Zhang and co-workers synthesized another copper-based water-resistant MOF, UPC-29, but this time using the ditopic H₂PC ligand (Figure 2) with high hydrophobic character.⁴² Another example where aromatic phenyl-rich hydrophobic linkers have been used to prepare hydrophobic MOFs was reported in 2017 by Chen et al., who used the octatopic linker H₈TDHB (3,3',5,5'-tetrakis(3,5-dicarboxyphenyl)-2,2',4,4',6,6'-hexamethylbiphenyl; Figure 2).⁴³ The authors reported a copper-paddlewheel MOF (BUT-155) composed of H₈TDHB.⁴³ Unlike previous copper-paddlewheel-based MOFs, such as HKUST-1 (also known as MOF-199), BUT-155 showed high stability in water, retaining its structure even after treatment in boiling water for 10 days. Furthermore, the authors highlighted the potential of this MOF to extract aniline vapor in preference to other organic and water vapors, which was attributed to its acidic property due to open metal sites in its structure and high hydrophobicity, respectively.⁴³

He et al. have reported an organotin-based MOF (SnTCPP-SHE) with superhydrophobicity.⁵³ The Sn-based MOFs were synthesized solvothermally with various Sn-based ligands and a TCPP linker and have demonstrated a WCA of up to 170° due to the hydrophobic nature of organotin building units. Additionally, the SnTCPP-SHE MOF has shown a surface area of 3940 m² g⁻¹, which is among the highest BET surface areas reported to date for hydrophobic MOFs.

In another study, Kitagawa et al. reported a superhydrophobic porous coordination polymer (PCP) with high roughness and low-energy surfaces.⁵⁴ The coordination polymer was formed by reacting Zn(NO₃)₂·4H₂O with the organic linker 1,3,5-tris(3-carboxyphenyl)benzene (H₃BTMB).

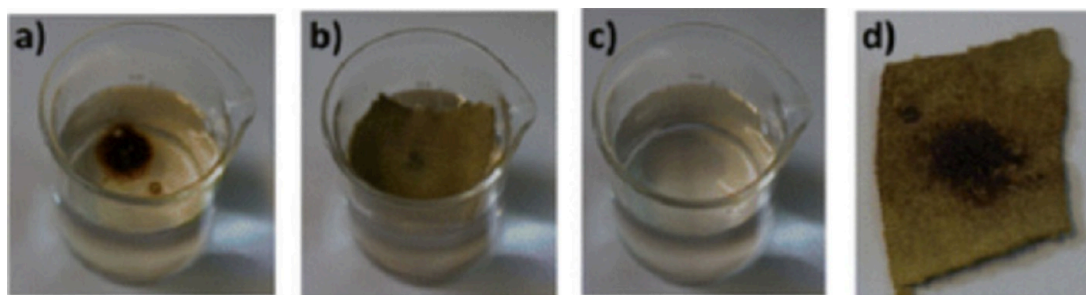


Figure 4. (a) Sample of crude oil/water mixture. (b) HEX-MOF@cotton composite applied on the surface of the mixture. (c) Successful removal of crude oil. (d) HEX-MOF@cotton fabric after oil sorption. Adapted with permission from ref 56

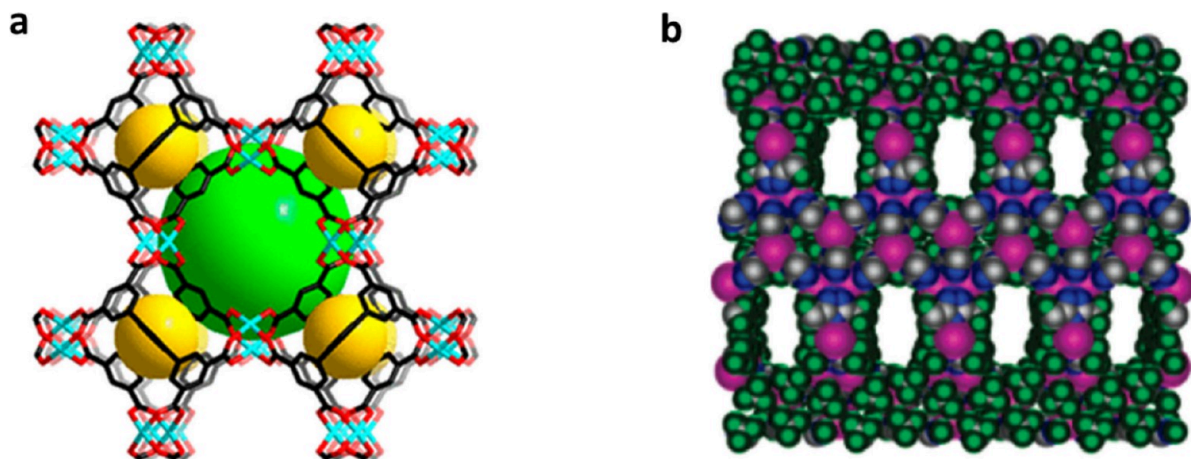


Figure 5. Framework structure of (a) Cu-paddle-wheel-dhb⁸⁻ MOF (BUT-155) (adapted with permission from ref 43) and (b) fluorous MOF (FMOF-1) (adapted with permission from ref 48).

As is shown in Figure 3, the crystalline nature of the PCP results in terminal phenyl moieties that create “microtextures”, resulting in a WCA of $>150^\circ$. The strategically selected low-symmetry linker resulted in a large area of the crystal surface being covered by the phenyl rings, which contributed to the hydrophobic properties of the MOF.

As shown in the above studies, the choice of the linker greatly influences the hydrophobicity of the resulting MOFs. Interestingly, in 2016 researchers synthesized a novel MOF with switchable hydrophobic and hydrophilic behavior.⁵⁵ The Zn-based MOF was assembled from a 1,4-benzenedicarboxylate and carborane-based linker. With the enhanced hydrophobicity of the carborane linker, the MOF powder exhibited a WCA of 140° .

In 2017, Sun and co-workers⁴¹ prepared a Cu-paddle-wheel MOF, UPC-21, using the pentiptycene tetracarboxylic acid as a hydrophobic linker. UPC-21 showed excellent hydrophobicity with a water contact angle of 145° . Additionally, UPC-21 exhibited excellent separation efficiency (99%) for various oil/water mixtures such as toluene/water, hexane/water, gasoline/water, and naphtha/water. However, a lower efficiency was observed for the crude oil/water mixture, which was attributed to its high viscosity and multicomponent nature. In 2019, Zhang and co-workers⁴² reported the synthesis of another Cu-paddle-wheel-based MOF, UPC-29, in which the authors used a pentiptycene ditopic linker instead of the tetratopic linker used in UPC-21, resulting in UPC-29 with a high water contact angle of 178° indicating excellent hydrophobic behavior, though no oil adsorption capacity has been reported for this material.

Another strategy to build hydrophobic MOFs is to use organic linkers bearing long alkyl chains. In 2016, Maji and co-workers were reported the use of a dialkoxyoctadecyl-oligo-(*p*-phenyleneethynylene)dicarboxylate (OPE-C18) linker (Figure 2) to prepare a Zn-based three-dimensional hydrophobic MOF (NMOF-1).⁴⁷ Interestingly, the octadecyl alkyl chain (C18) present in this MOF protruded outward from the 1D chain of Zn-OPE-C18. Structural characterization of this MOF also revealed that π - π stacking between the chains allowed the formation of a 2D structure, whereas the 3D structure was built out via interactions between alkyl chains. This led to the formation of NMOF-1 with reduced surface free energy and a WCA of 160 – 162° , indicative of the superhydrophobicity of this MOF. Furthermore, NMOF-1 showed self-cleaning behavior with retained superhydrophobicity over a pH range of 1–9 in a concentrated ionic medium.⁴⁷

Another strategy to induce hydrophobicity is to integrate long-chain alkyl groups as part of the linkers. For example, in a study by Manos et al. the use of long-chain alkyl-functionalized amino terephthalic acid linkers for Zr-based MOFs was investigated.⁵⁶ The aminoterephthalic acid linker was reacted with various alkylaldehydes to form alkyl-functionalized amine derivatives, which were then used to synthesize Zr-based MOFs. The derived MOFs showed an unusual Zr(IV) 6-c net as a result of steric hindrance caused by the alkyl groups. The MOFs have shown hydrophobic properties, with WCAs ranging from 150° to 154° , except for the hexyl-amino- H_2BDC MOFs, which showed wettability to water. The MOFs and their composites with cotton fabrics showed efficient

separation of crude oil from water in both static and continuous flow modes (Figure 4).

Another class of hydrophobic MOFs is fluorine-functionalized MOFs (F-MOFs). In this class of MOFs, fluorine is integrated into the MOF either by incorporating it within the inorganic metal cluster of the MOF or through the use of fluorine-rich organic linkers. Fluorine-functionalized organic molecules are often hydrophobic and are stable against oxidation, making them highly sought after due to their stability.⁵⁷ Early reports of F-MOFs can go back to 2007 when Omary and co-workers utilized the perfluorinated 3,5-bis-(trifluoromethyl)-1,2,4-triazolate ligand (Tz, Figure 2) to synthesize a class of Ag(I)-based fluorine-functionalized MOFs (FMOF-1 and FMOF-2).^{48,58} These highly fluorinated MOFs contain a tubular channel with [Ag₄Tz₆] clusters (Figure 5). The authors have reported that FMOF-1 and FMOF-2 displayed high adsorption toward various liquid hydrocarbons, such as *n*-hexane, cyclohexane, benzene, toluene, and *p*-xylene, in preference to water, with FMOF-2 showing a toluene adsorption capacity double that of FMOF-1 due to its larger pore size.⁴⁸

In 2013, Miljanić et al.⁴⁹ used the perfluorinated aromatic linkers F1–F3 (Figure 2) to synthesize copper-based hydrophobic MOFs (MOFF-1, MOFF-2, and MOFF-3). MOFF-1 was prepared by combining the 2,2',3,3',5,5',6,6'-octafluorobiphenyl-4,4'-dicarboxylic acid (H₂OFBPDC) linker with Cu(NO₃)₂ in a solvothermal reaction, producing 2D methanocapped layers of Cu₂OFBPDC. While MOFF-2 was made of the same dicarboxylic ligand (H₂OFBPDC), diazabicyclo[2.2.2]octane (DABCO) was used as a pillar to interconnect the 2D Cu₂OFBPDC layers, forming a three-dimensional network (Figure 6). Similarly, the tetrazole-based

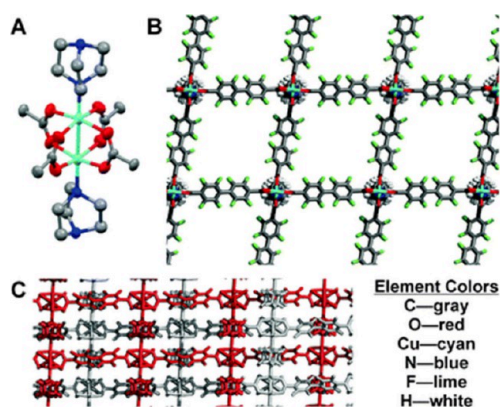


Figure 6. X-ray crystal structure of MOFF-2. (A) Secondary building unit of MOFF-2. (B) View along the one-dimensional channels in MOFF-2. (C) Side-on view of MOFF-2 with two independent nets shown in different colors. Adapted with permission from ref 49.

linker H₂PFBPTZ (Figure 2) was used to synthesize MOFF-3, bearing a one-dimensional hydrophobic channel in its structure. Contact angle measurements revealed that MOFF-1, MOFF-2, and MOFF-3 are all hydrophobic with WCA = 108 ± 2°, 151 ± 1°, and 134 ± 2°, respectively. In contrast to MOFF-1 and MOFF-3, MOFF-2 crystallizes with no water molecules in its pore voids, another indication of its superhydrophobic behavior.⁴⁹

3.2. Post-Synthetic Modification of MOFs for Improved Hydrophobicity. Post-synthetic modification (PSM) is another strategy widely used to introduce hydrophobicity in

MOFs. PSM involves modifying the structure of MOFs via alteration in the metal centers or linkers by treating the MOFs with suitable reactants. For example, long alkyl chains, aromatic rings, or fluorinated groups can be added by post-synthetic treatment of MOFs to introduce hydrophobicity in the structure. This can be achieved either by (i) coordinating an unsaturated metal site (open metal site) with a ligand containing hydrophobic functional groups or terminal long alkyl chains or (ii) chemical transformation/derivatization of the functional groups in the organic linker, such as functional transformation of an amino group (–NH₂) into an amide group (R–CO–NH₂), where R is a long alkyl chain typically with 4–12 carbon atoms. The main advantage of PSM is that it allows for the diverse functionalization of the MOFs without interfering in their core structure as opposed to optimization of the structure of the MOFs during synthesis, which is often more challenging.⁵⁹ An example of oxo-metal cluster decoration can be found in a study done by Sun et al.⁶⁰ In this study the oxo cluster of UiO-66-NH₂ was post-synthetically modified via grafting of a hydrophobic phenylsilane (PhSiH₃) by reacting it with the Zr–OH groups. This addition of a hydrophobic phenyl group resulted in the formation of a superhydrophobic MOF system with a WCA of 161°. The phenylsilane-modified MOFs showed excellent resistance to degradation against acid and basic environments compared to UiO-66-NH₂. To investigate the efficiency of the MOF for separation, the MOF was deposited on a stainless-steel mesh to form a separation filter (Figure 7).

Another example of utilizing the vacant uncoordinated metal sites for PSM was reported in 2019 by Han and co-workers,⁶¹ who attached octadecylamine (OA) with the open coordination sites present in the activated MIL-101(Cr), UiO-66, ZIF-67, and HKUST-1 to form superhydrophobic MOFs (S-MOFs) (Figure 8). The prepared MOFs retained their crystallinity and morphology as confirmed by PXRD and SEM. Furthermore, S-MIL-101 (Cr) displayed enhanced superhydrophobic properties with a relatively high-water contact angle (156°) and less water absorptivity. The surface-modified S-MIL-101 (Cr) MOF exhibited separation capacities of 118–281 and 142–369 wt % for the pristine MOF and its functionalized counterpart, respectively.

In addition to modifying the uncoordinated metal sites of the MOF structure, the ligand can also be post-synthetically modified by addition of hydrophobic functional groups. It was shown that amine-functionalized linkers are susceptible to post-synthetic modification and often used to introduce hydrophobic properties. Nguyen et al. have post-synthetically modified the isoreticular series of IRMOFs and MIL-53(Al)⁶² through the addition of medium to long alkyl chains. The hydrolytic stability of the MOFs was assessed by exposure to ambient air and submersion in water for up to 4 days. The added hydrophobicity not only increased the WCA but also helped to stabilize the MOF against degradation, which was evidenced by comparing the PXRD patterns of the samples. Based on the same MOF, Xue et al. grew flower-like MOF-53-OH on a polyacrylonitrile/polyethylenimine (PAN/PEI) membrane to enable the separation of oil from an oil/water emulsion as well as the removal of soluble dyes.⁶³ The introduced PAN layer allowed the organic linker in MOF-53-OH to cross-link on the membrane surface, making it superhydrophilic with a high uptake capacity.

Lui et al. developed a superhydrophobic ZIF-90 by performing post-synthetic modification on the pristine ZIF-

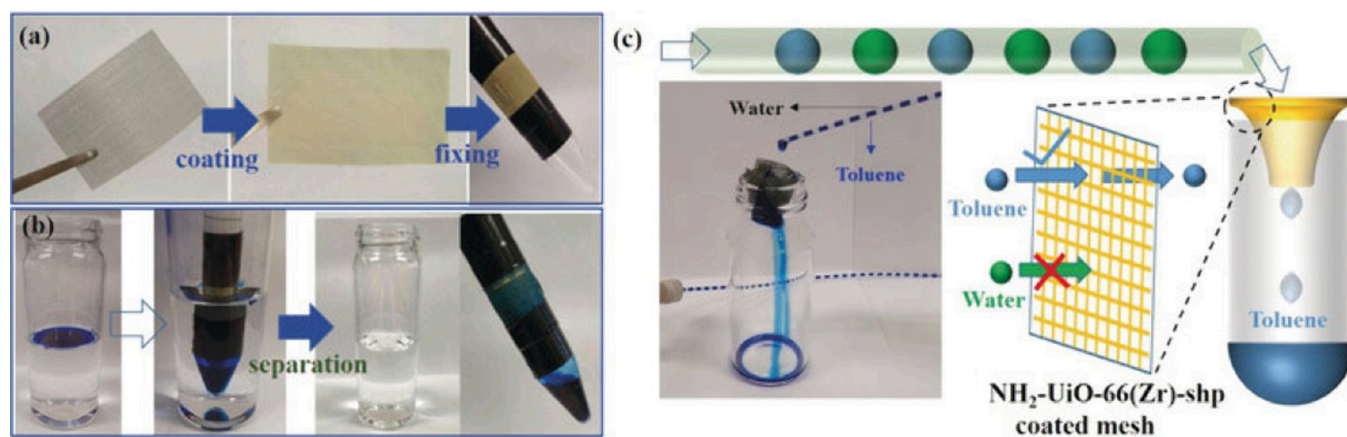


Figure 7. (a) Preparation of a separator by assembling superhydrophobic MOF ($\text{NH}_2\text{-UiO-66(Zr)-shp}$) coated stainless mesh with a test tube collector and (b) selective separation of Oil Blue N labeled toluene from water. (c) Schematic illustration and photograph of the continuous separation of toluene from alternating droplets of water/toluene. Reproduced with permission from ref 60.

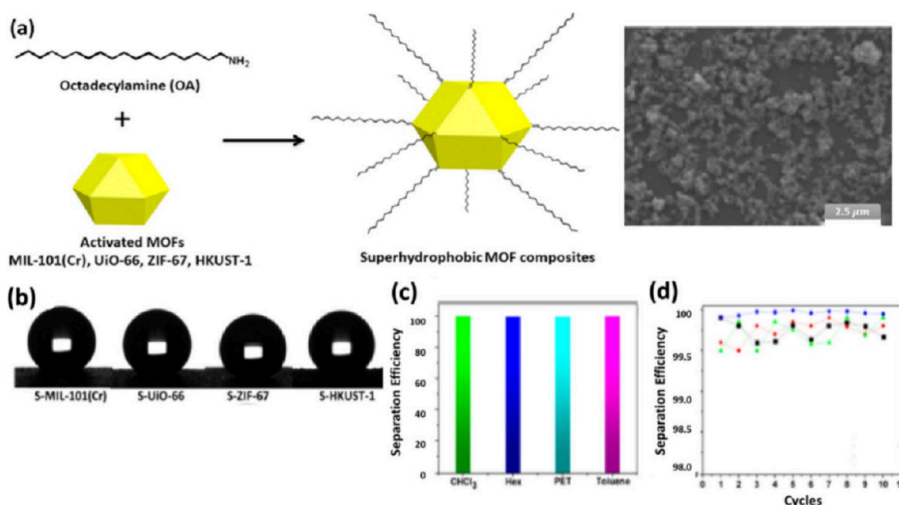


Figure 8. (a) Schematic illustration of the formation of surface-modified superhydrophobic MOF composites using the octyadecylamine amine coordinating ligand. The SEM image shown on the right presents the surface modified S-MIL-101(Cr). (b) Water contact angles of surface-modified MOF composites. (c and d) Separation efficiency of S-MIL-101(Cr) composites for separating oil form different kinds of water–oil mixtures (green, CHCl_3 ; blue, hexane; cyan, PET; and red, toluene). Adapted with permission from ref 61.

90 to develop a reusable adsorbent of bioalcohol from water mixtures.⁶⁴ Functionalization of ZIF-90 with pentafluorobenzylamine was performed through an amine condensation reaction in which the pentafluorobenzylamine was reacted with the aldehyde group of the ZIF-90 imidazolate-2-carboxyaldehyde linker. The fluorinated ZIF-90 showed a WCA of 152.4° compared to that of 93.9° for nonfunctionalized ZIF-90. The improved hydrophobicity was attributed to the incorporation of the fluorinated pentafluorobenzylamine within the MOF structure introduced by PSM. Additionally, the MOFs were tested for their hydrolytic and thermal stability by boiling them in water for 24 h. The MOFs showed high chemical and thermal stability. As evidenced by thermal gravimetric analysis (TGA), both the fluorinated and as-prepared ZIF-90 showed a similar plateau region in the temperature range of $80\text{--}300^\circ\text{C}$ without significant weight loss, even after the measurement of water stability.

4. MOF COMPOSITES FOR OIL/WATER SEPARATION

While many studies have been focused on the development of intrinsically hydrophobic MOFs for the separation of oil and

water, there is a growing interest in the development of MOF composites for the enhancement of their properties and extending their applicability. It also takes advantage of integrating desirable properties of the MOFs and the other components (such as the polymer) of the composites. MOF composite membrane materials include mixed matrix membranes, where the MOF acts as a filler in a continuous polymer matrix; polycrystalline membranes, in which a thin crystalline layer of a microporous MOF is deposited on a substrate material for mechanical support; and nanosheet membranes, derived from the fabrication of thin MOF membranes by the layer-by-layer deposition method. Other popular composite materials include incorporating MOFs into structures bearing high surface areas and large pores such as highly fluorinated graphene oxide (HFGO)^{30,51} or environmentally friendly materials, such as cotton,⁶⁵ cellulose,^{38,66} carbon sponges,⁶⁷ biodegradable melamine,^{39,68} and polylactic acid (PLA)^{69,70} Considerable efforts have recently been made to improve the recyclability and environmental compatibility of the MOF–polymer composites. For example, MOFs have been incorporated into biodegradable matrices, such as PLA and

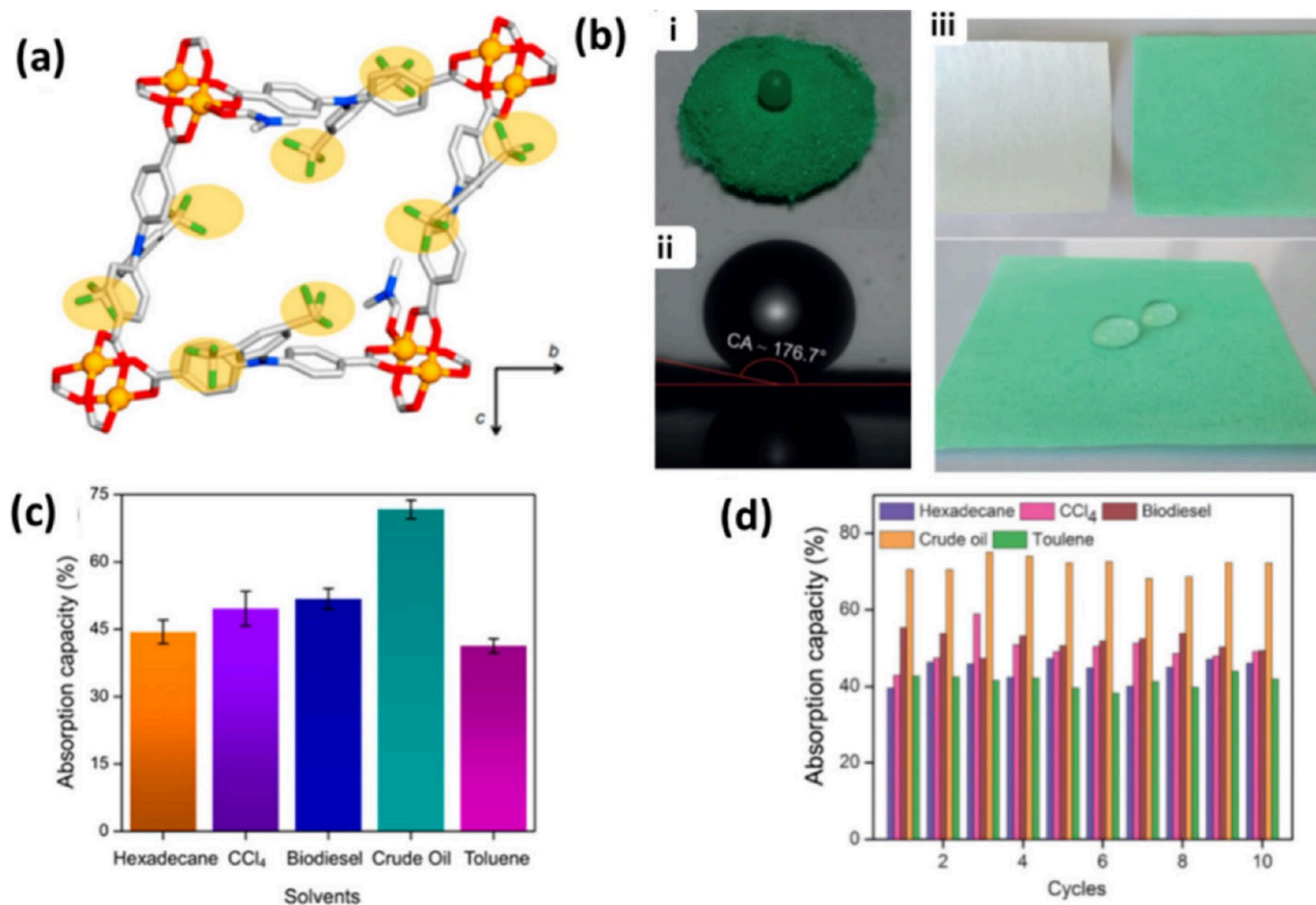


Figure 9. (a) View of single fluororous pores of UHMOF-100 with CF₃ groups highlighted in yellow. (b) (i) Photographs of a water droplet suspended on UHMOF-100, (ii) water contact angle of UHMOF-100, and (iii) photographs of the membrane base (white) and MOF-coated membrane (green) and (bottom) retention of hydrophobicity for the MOF-coated membrane. (c) Absorption capacities and (d) recycling tests of UHMOF-100/PDMS/PP. Adapted with permission from ref 52

other polymers (see below), to improve the stability and environmental compatibility of the MOFs and simultaneously improve the oil separation performance of the polymer using the properties of the incorporated MOF, such as hydrophobicity, surface area, and tunable porosity. In 2016, Ghosh and co-worker reported the “first” ultrahydrophobic Cu-based MOF, [(Cu₄L₄(DMF)₄)(DMF)₃]_n (UHMOF-100) (Figure 9), using 4,4'-([3,5-bis(trifluoromethyl)phenyl]azanediyl) benzoic acid (H₂L = H₂TFPBA, Figure 2) as a linker with fluorine-rich CF₃ groups.⁵² The excellent water-repellent and high oil-absorptivity characteristics of this MOF were evidenced by the very high water contact angle (176°) and low oil contact angle (0°). The MOF was spray-coated on a reusable polypropylene support using polydimethylsiloxane (PDMS) as a binding agent to design a membrane for water/oil separation. However, compared to the pristine MOF, the resulting composite UHMOF-100-PDMS-PP showed a lower WCA (135°), which was attributed to the PDMS with its lower WCA of 109°. Generally, the membrane retained a high level of hydrophobicity and oleophilicity, with good separation capacity for various kinds of oil/water mixtures for toluene, hexadecane, chloroform, biodiesel, and crude oil/water mixtures ranging between 40 (for a toluene/water mixture) and 75 wt % (for crude oil/water mixture).

Another strategy for introducing hydrophobicity into the composite is using a hydrophobic substrate as a support for

MOFs. Fisher and co-workers used this strategy and reported the development of a hydrophobic/oleophilic zeolite imidazole framework (ZIFs) composite in 2016.³⁰ The group reported the synthesis of superhydrophobic/superoleophilic monocrystalline ZIF-8 composites (HFGO@ZIF-8) prepared using a highly fluorinated graphene oxide substrate. The oxygen functionality of the graphene surface allowed both selective nucleation and control over ZIF-8 crystal growth, resulting in the intercalation of the ZIF-8 network between HFGO layers. The resulting composite displayed a high WCA of 162° compared to the WCAs of 56° and 125° for the pristine ZIF-8 and HFGO, respectively. The composite showed a low contact angle of 0° for oil, indicating its superoleophilic nature. The relative absorption capacity for the pristine ZIF-8 was reported between 10 and 150 wt % for different types of oils and organic solvents, whereas the HFGO@ZIF-8 composite showed enhanced capacity with a range of 20–280 wt %. The group investigated further and fabricated a sponge@HFGO@ZIF-8 composite, in which a commercial sponge was immersed overnight in the reaction mixture containing all components of the HFGO@ZIF-8 composite. The resulting sponge@HFGO@ZIF-8 hybrid composite achieved 150–600 wt % oil absorption capacity for various mixtures, including vegetable oil, heptane, DMF, and chloroform. Interestingly, the sponge readily floats on water, permitting scalable practical application of this material.

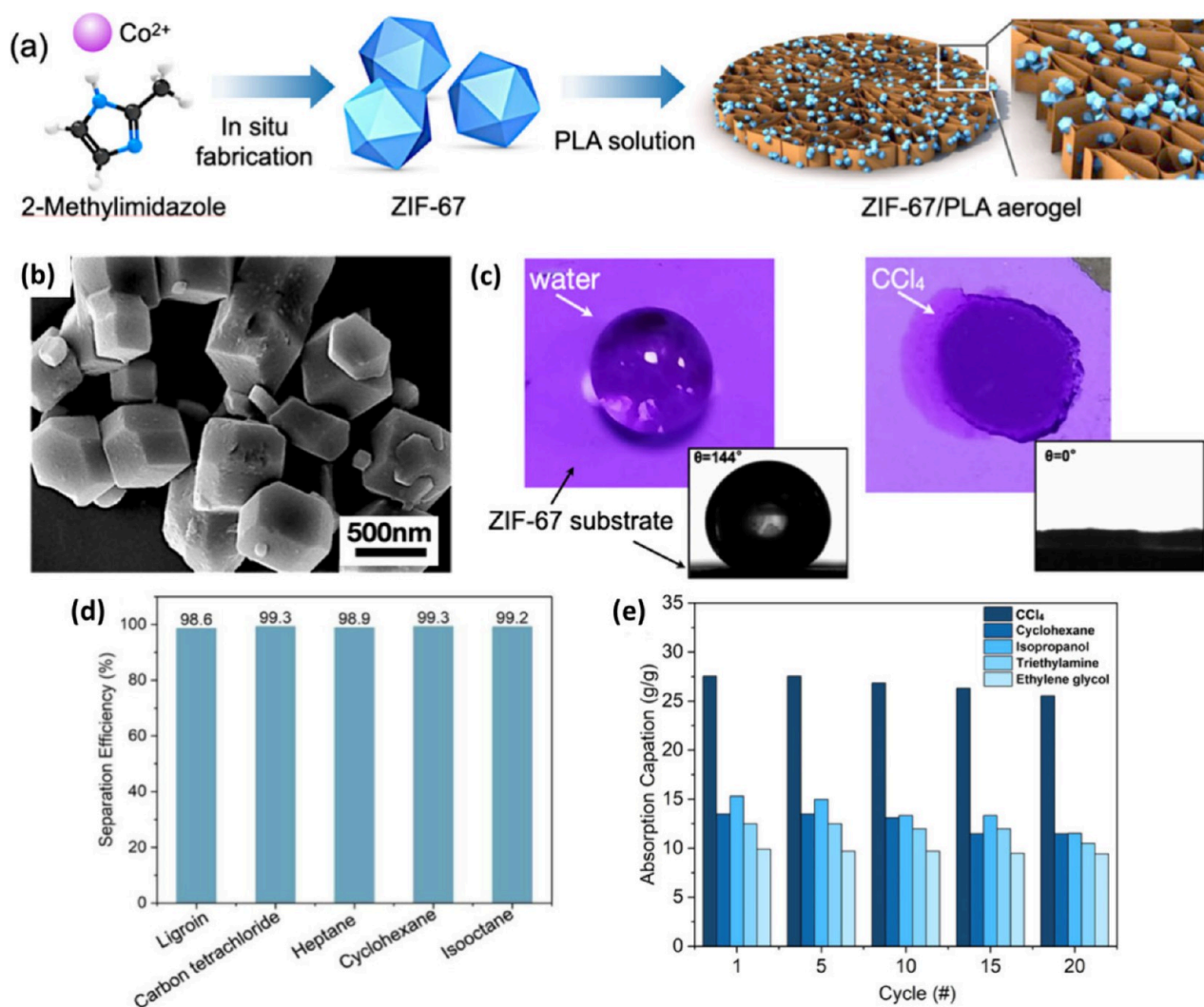


Figure 10. (a) Schematic showing the preparation of the ZIF-67@PLA aerogel/composite with a honeycomb structure. (b) SEM image of ZIF-67, (c) digital images with corresponding CA measurement of the ZIF-8 substrate with a drop of water (144°) and a drop of CCl_4 (0°), (d) separation efficiency, and (e) adsorption capacity with cycle test of the ZIF-67@PLA aerogel/composite for different oil/water mixtures. Adapted with permission from ref 70.

More recently, ZIF-8 was also incorporated into a melamine formaldehyde (MF) composite for oil/water separation.⁷¹ The ZIF-8@MF composite was produced by an in situ deposition method. Despite the hydrophilicity of the MF substrate (WCA 54°), the ZIF-8@MF composite displayed high WCA (145°) and very low oil CA of 0° , indicating the superhydrophobicity and superoleophilicity of the resulting composite. Furthermore, the ZIF-8@MF composite achieved adsorption capacities in the range of 68–165 wt % for various oil/water mixtures, with a separation efficiency of around 100% for up to 20 cycles.

Due to their attractive biodegradability and recyclability, poly(lactic acids) (PLAs) have found applications in a variety of composite materials. However, PLA matrices still have limited oil adsorption capacity and poor mechanical properties that limit their wide application in oil/water separation. Due to its high hydrophobicity and superoleophilicity (oil CA 0°), ZIF-8 was also incorporated into biodegradable PLA by solvent-assisted dispersion using sonication and mixing, followed by freeze-drying.⁶⁹ In 2021, Li et al. combined ZIF-8 nanoparticles with a PLA matrix using physical mixing to

produce a ZIF-8@PLA composite. The pore size, surface roughness, and surface area of the resulting ZIF-8@PLA composite were successfully tuned by changing the ratio of ZIF-8 in the PLA polymer matrix. In addition, the resulting ZIF-8@PLA composite exhibited improved oil separation performance and significantly improved mechanical properties compared with those of the virgin PLA polymer.

The resulting composite ZIF-8@PLA showed a WCA of 145° and successfully separated the mixtures of oil/water, heptane/water, carbon tetrachloride/water, and pentane/water with a separation capacity range of 15–30 wt %, a flux range of $13000\text{--}35000\text{ L m}^{-2}\text{ h}^{-1}$, and an efficiency of around 100% for up to 20 cycles.

In another study using a similar method, PLA was formulated with ZIF-67 to produce a honeycomb ZIF-67@PLA composite for oil/water separation (Figure 10).⁷⁰ A typical optimized loading of 3 wt % ZIF-67 in PLA produced the ZIF-67@PLA composite with the highest wettability, displaying a WCA of 132° compared to that of 107° for the PLA on its own. The composite showed a moderate adsorption capacity (10–25 wt %) with a good flux range ($51180\text{--}71660$

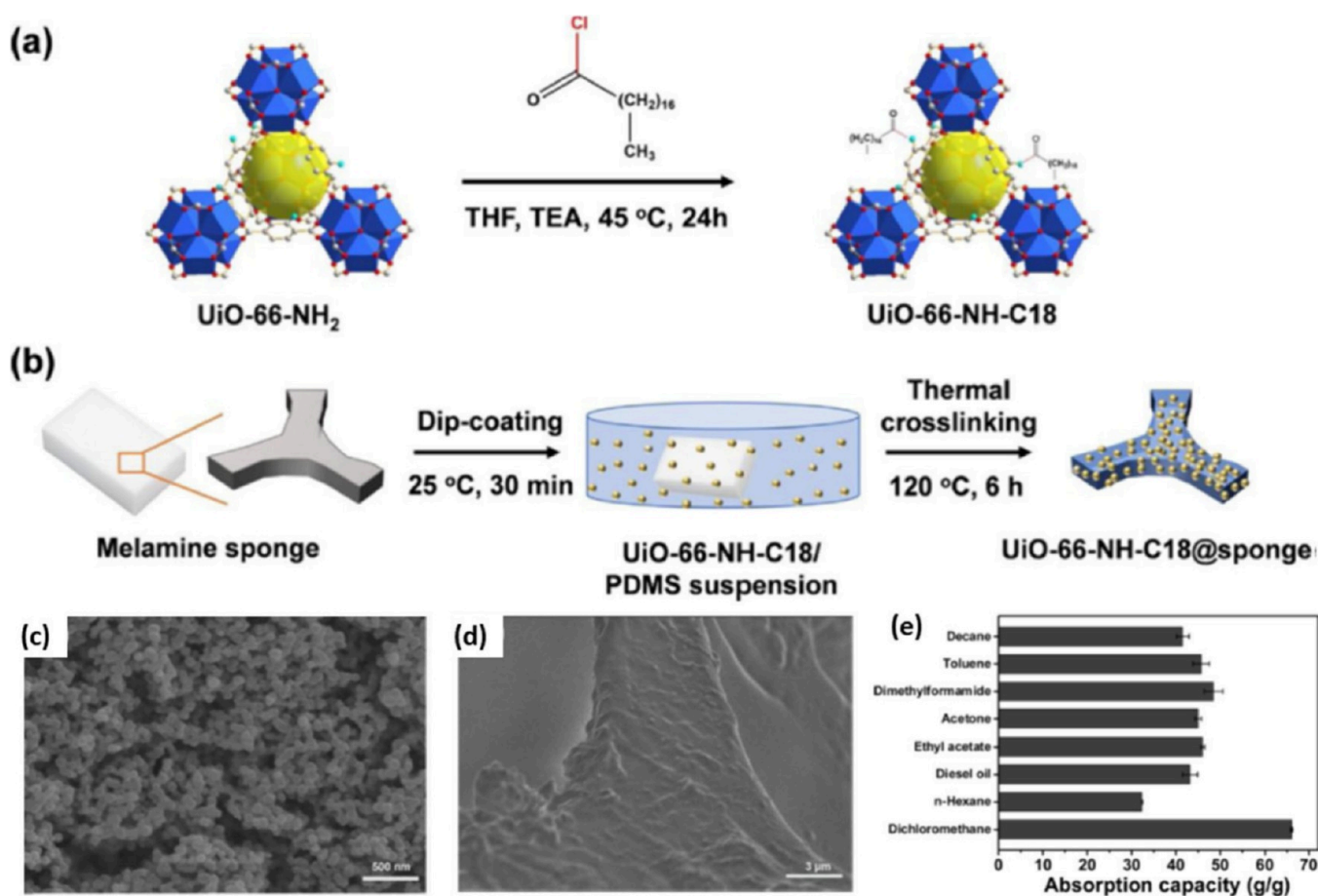


Figure 11. Schematic showing the preparation of (a) superhydrophobic UiO-66-NH-C18 and (b) its composite UiO-66-NH-C18@sponge. (c, d) SEM images of UiO-66-NH-C18 and its composite UiO-66-NH-C18@sponge. (e) Absorption capacity bar chart of the UiO-66-NH-C18@sponge composite for various kinds of organic/water mixtures. Adapted with permission from ref 32.

L m² h⁻¹) and excellent separation efficiency (~98–100%), and usability was tested for 20 cycles for petroleum ether/water, carbon tetrachloride/water, heptane/water, cyclohexane/water, and isooctane/water mixtures.

Huang and co-workers prepared a hydrophobic MOF, UiO-66-NH-C18, by amidation of the amino group of UiO-66-NH₂ with octadecanoyl chloride (Figure 11).³² Owing to the long alkyl chain covalently attached to the surface of the MOF, the resulting UiO-66-NH-C18 showed superhydrophobic properties with a high WCA of 152°. UiO-66-NH-C18 adsorbs much less water than the pristine UiO-66-NH₂ (28% of that for UiO-66-NH₂). Furthermore, the group prepared a superhydrophobic composite, UiO-66-NH-C18@sponge, by dip-coating a melamine formaldehyde sponge with UiO-66-NH-C18. This composite was found to display an enhanced absorption capacity ranging between 32.3 and 66.1 wt % for various oils and organic solvents.

Biswas et al.⁵⁰ synthesized a hydrophobic Hf-based MOF (SHMOF). In situ coating of SHMOF on polypropylene (PP) fabric produced a superhydrophobic SHMOF@PP fabric composite (Figure 12) with a WCA of 160°, high separation efficiency (93–99%), good recyclability (up to 20 cycles), and moderate absorption capacity (29–39 wt %) for separating crude oil from an oil/water mixture. The same group synthesized a hydrophobic Zr-based MOF (1'@CF₃) through post-synthetic modification of the free hydroxyl groups in the UiO-66-OH (1') by attaching OCCF₃ groups.⁶⁸ The stability

of the MOFs was tested by stirring them at room temperature for 24 h in water acquired from various sources (river, pond, tap, and seawater) at a broad pH range of 2–14. PXRD patterns of the treated samples were compared with those of the pristine MOFs, and their identical patterns indicated excellent stability. The resulting hydrophobic MOF was utilized in the preparation of a robust melamine-based composite (1'@CF₃@melammine) using polymethylhydrosiloxane (PMHS) to help anchor the prepared MOF on the melamine sponge. The resulting 1'@CF₃@melammine composite showed a WCA of 145° compared to that of 104° for the polymeric material alone. The absorption capacity and separation efficiency were reported as 27–37 wt % and 95–99% for the MOF alone (1'@CF₃) and the composite (1'@CF₃@melammine), respectively. Furthermore, 1'@CF₃@melammine was tested successfully for separation of the oil/water mixture for up to 50 cycles.

Additionally, The same group used a nonfluorous long-carbon linker, palmitadodoterphtalic acid, to prepare a superhydrophobic MOF, SH-UiO-66.³⁹ SH-UiO-66 was deposited on a melamine-based sponge using the PDMS-PHDMS cross-linking agent. The resulting composite SH-UiO-66@sponge showed almost the same WCA as the pristine MOF (168°), indicating the superhydrophobic nature of both the MOF and the composite. The SH-UiO-66@sponge composite displayed a good oil/water separation efficiency

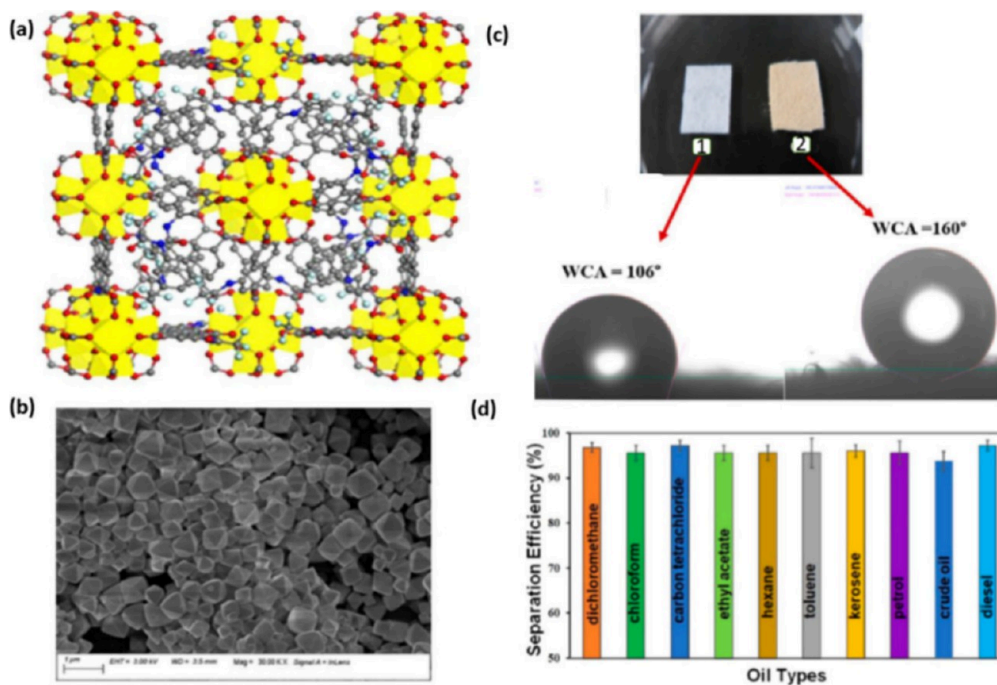


Figure 12. (a) Simulated crystal structure of SHMOF (Zr polyhedron; C, O, N, and F are displayed in yellow, gray, red, and blue, respectively). (b) SEM image of SHMOF. (c) WCA value of (1) native polypropylene (PP) fabric (106°) and (2) SHMOF-PP composite (160°) with increased hydrophobicity due to the immobilization of SHMOF onto the PP fabric. (d) Separation efficiency (%) of the SHMOF-PP composite for various oil/water mixtures. Reproduced with permission from ref 50.

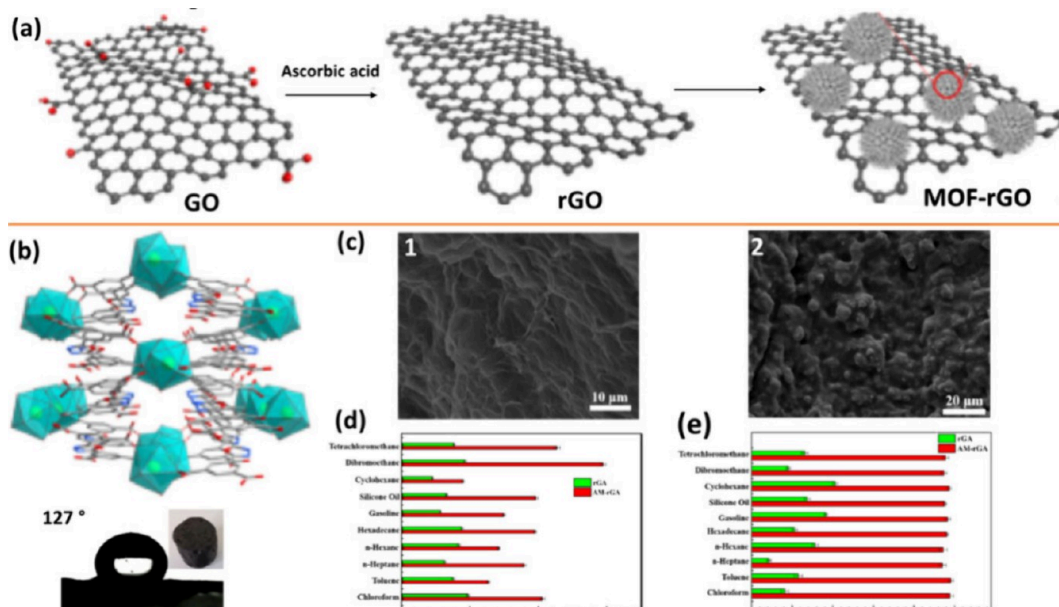


Figure 13. (a) Proposed scheme for the self-assembly process of rGO and amylamine-modified (Eu-bdo-COOH) MOF microspheres (one is highlighted with a red circle). (b) 3D framework of Eu-bdo-COOH MOF with the water contact angle (127°). (c) SEM images of (1) rGO and (2) MOF-rGO. (d) Adsorption capacities and (e) separation efficiencies of MOF-rGA and rGA toward 10 different types of oil/water mixtures. Reproduced with permission from ref 51

range between 43.8 and 97.2 wt % and a flux range of $58263\text{--}47416\text{ L m}^{-2}\text{ h}^{-1}$ for various oil/water mixtures (see Table 1).

The mesoporous iron-based MOF MIL-100 was transformed into its porous carbonaceous form, PC-MIL-100(Fe), by Cabello and co-workers.⁷² Incorporation of PC-MIL-100(Fe) into a commercially available melamine-formaldehyde sponge (MFS) resulted in a highly hydrophobic and oleophilic composite sponge MFS-PC-MIL-100(Fe). The composite

showed a WCA of 145° and 0° oil contact angle. The absorption capacity of the MFS-PC-MIL-100(Fe) composite for various oils was in the range of 10–17%, showing stability up to 17 cycles. It is worth noting that this composite was fabricated by the simple dispersion of PC-MIL-100(Fe) into melamine-formaldehyde sponges.

Control of crystal morphology combined with post-synthetic modification has also been used to control the hydrophobicity

of MOFs, followed by their integration into composites. According to a report by Fan and Yang et al., adjusting the crystallization process changes the morphology of the Eu-bdo-COOH MOF from hexagons to microspheres, resulting in enhanced hydrophobicity.⁵¹ The resulting MOF, Eu-bdo-COOH (Figure 13), displayed high stability in a broad pH range and at high temperatures up to 400 °C. In order to modify the hydrophobicity of the resulting MOF, free “hydrophilic” carboxylic acid groups (WCA = 32°) were transformed into “hydrophobic” alkyl groups through post-synthetic modification of the Eu-bdo-COOH MOF via reaction with a series of alkylamines (ethylamine to octylamine) to produce amyl-MOFs (A-MOFs) displaying a water contact angle of 142°, indicating a high degree of hydrophobicity for the modified MOF. The group combined the hydrophobic amyl-MOFs with reduced graphene oxide (rGO) to produce an A-MOF-rGA composite for oil/water separation. The A-MOF-rGA composite displayed a somewhat reduced WCA angle (127°) due to the very low hydrophobicity of the rGO within the composite, exceptional absorption efficiency for various oil/water mixtures, including an impressive absorption capacity of 14 728 wt % for a dichloromethane/water mixture, and 100% separation efficiency without any decay in performance after 50 cycles.

Hydrophobic composites can take advantage of the hydrophobicity of one or more of the components of a composite. In a study by Zhang et al., ZIF-8 was loaded on top of oxidized carbon nanotubes (CNTs) to create a composite, ZIF-8@CNT, for the effective separation of oil/water emulsions.⁷³ The oxidized CNT provided nucleation sites for the growth and deposition of ZIF-8 particles. The composite was tested for its demulsification ability on an oil/water mixture made from brine and crude oil. As shown in Figure 14, the composites had high oil removal rates over 30 min,

reaching a maximum of 99.4%. The composite functions by replacing the emulsifier at the oil/water interface, bridging oil droplets to form larger ones. The mechanisms that contribute to such a high demulsification rate can be explained by the synergistic effects between ZIF-8 and the CNT structures. The imidazole ring and uncoordinated metal sites contribute to the oleophilicity of ZIF-8 and its high uptake. In addition, the surface charge on ZIF-8 caused by the positively charged metal centers can attract oil droplets via electrostatic attraction. Furthermore, the highly porous nature of the MOF allows for the adsorption of guest molecules. Highly conjugated structure of CNT facilitated π - π attraction between organic compounds. Hence, the enhanced ability to remove and separate oil from oil/water mixtures was observed as a result of the synergistic effects of the CNT and the MOF.

In another study by Han et al., a novel Zr-based MOF was deposited on polypropylene membrane to form composites with dual capability to separate oil/water mixture and function as a photocatalyst for cleaning organic pollutants.⁷⁴ The MOF composite was developed by the in situ growth of Zr-based MOFs, namely, DUT-52 and TF-DUT-52, from 1,4-naphthalenedicarboxylic acid (H₂NDC) and 1-trifluoroacetaminonaphthalene-3,7-dicarboxylic acid (H₂NDC-NHCOCF₃) as linkers, respectively. The DUT-52 and TF-DUT-52 composites showed WCAs of 132.5° and 156°, respectively. This enhanced hydrophobicity was attributed to the presence of trifluoroacetamide groups. The composite membranes showed >98% separation efficiency and a separation flux of >500 L m⁻² h⁻¹ bar⁻¹ for a cyclohexane and water emulsion in addition to >85% photocatalytic degradation efficiency under ultraviolet light, hence providing the composite with the capability for self-cleaning and treatment of organic pollutants.

As mentioned earlier, one of the key elements for the effective separation of oil/water mixtures is the selective filtration capability due to the superhydrophilic or superhydrophobic nature of the materials. Hence, working in reverse, superhydrophilic composites with underwater superoleophilicity have also been studied for oil/water separation by taking advantage of the surface morphology. Obaid et al. have synthesized a superhydrophilic iron-based MOF Cr-soc-MOF-1 composite by depositing the MOF on a cellulose ester substrate to create a hydrophilic composite.⁷⁵ The MOF composites were synthesized via vacuum-assisted self-assembly. The MOF membrane exhibited superhydrophilicity and underwater superoleophobicity, which enabled it to separate oil/water mixtures with more than 99.9% separation efficiency. Additionally, the composites showed high antifouling properties due to the synergistic effect of their surface roughness and superhydrophilicity. The composites also proved to be reusable for up to 10 filtration cycles. In another study, He et al. used the hierarchical nanostructure of Cu₂O₄ and HKUST-1 modified with fluoroalkylsilane for the fabrication of copper mesh membranes.⁷⁶ The MOF composite showed a separation efficiency of 94% in 165 min owing to the synergistic effect of adsorption and photocatalytic activity. The photocatalytic mechanism was mainly attributed to the generation of superoxide and hydroxyl radicals due to the action of the MOF composite as the catalyst. In another study by Ye et al., superhydrophilic hybrid membranes of UiO-66-NH₂ with poly(vinylidene fluoride) (PVDF), poly(vinyl alcohol) (PVA), and lauramidopropyl betaine (LPB) were fabricated.⁷⁷ The composite membrane possessed excellent hydrophilicity with a WCA of 2° and showed a high water flux of 15600 L m⁻² h⁻¹.

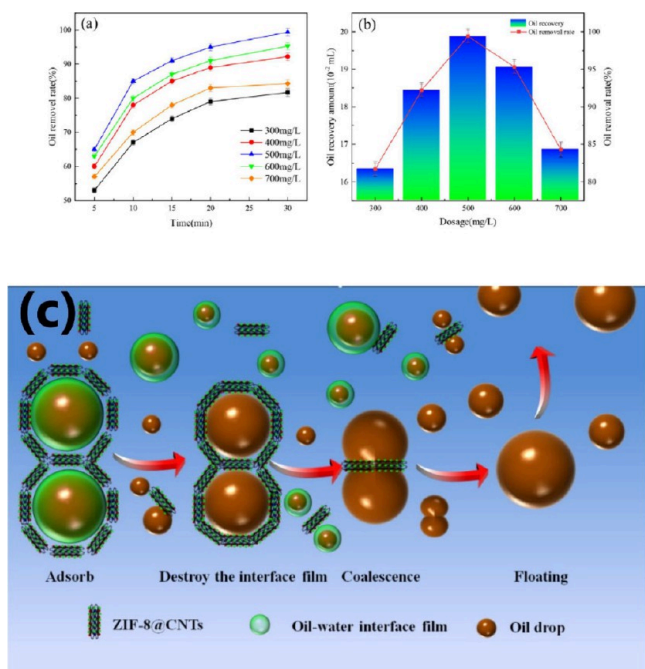


Figure 14. (a) Removal rate (%) of oil over a period of 30 min and (b) amount of oil recovery over dosage ranging from 300 to 700 mg/L. (c) The demulsifying mechanism of ZIF-8@CNT. Reproduced with permission from ref 73.

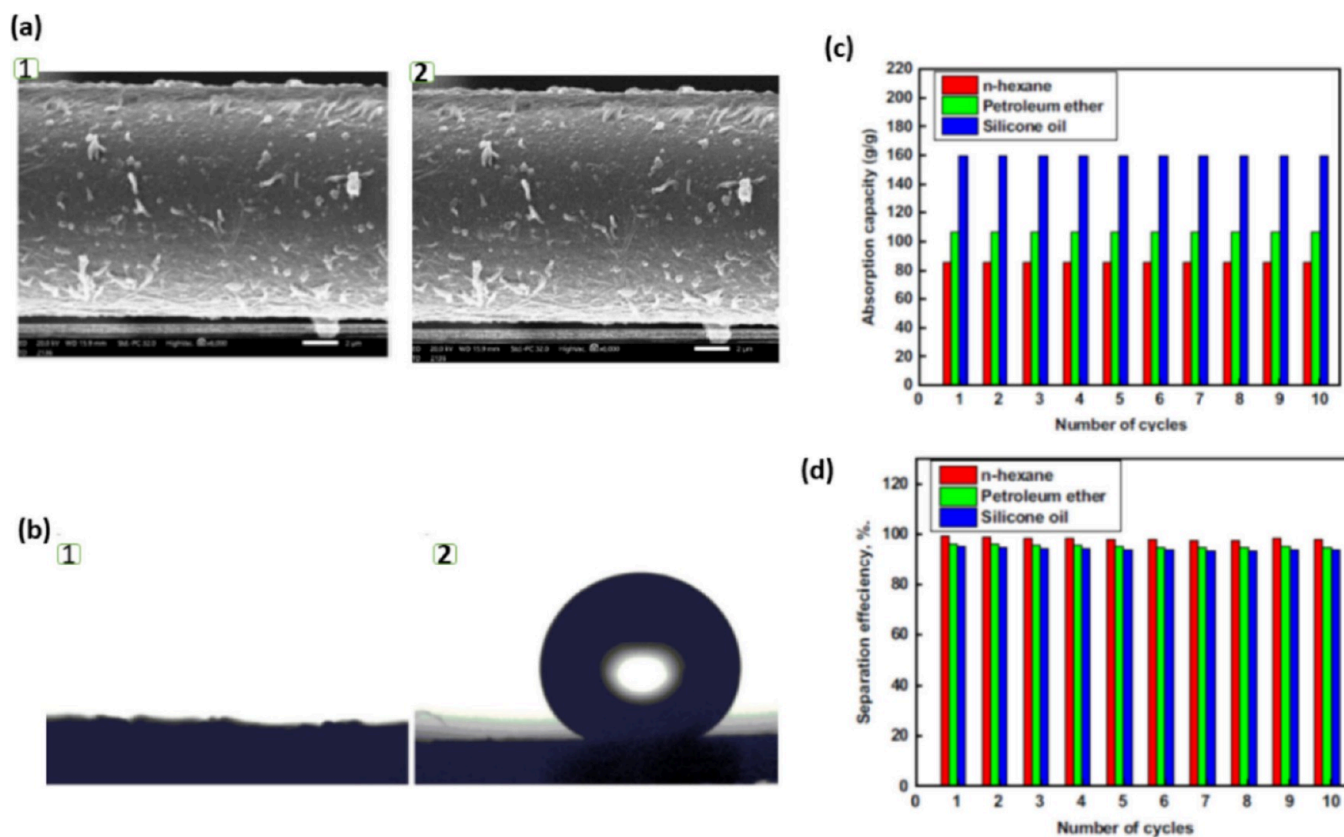


Figure 15. (a, b) SEM images of pristine textile fabric (1) and textile fabric modified by the Cu-Asp-MOF (2). (b) Images of a water droplet on (1) native pristine textile fabric ($\sim 0^\circ$) and (2) textile fabric by modified by the Cu-Asp-MOF (158°) with sharply increased hydrophobicity. (c) Absorption capacity and (d) separation efficiency of the modified textile fabric for different oil/water mixtures with up to 10 separation cycles. Adapted with permission from ref 33.

The composites also showed a high separation efficiency of 99%, in addition to the ability to filter bacteria and a self-cleaning ability.

5. BIODEGRADABLE MOF COMPOSITE FOR OIL/WATER SEPARATION

The majority of organic linkers used to construct the MOFs are not of natural origin and are synthesized through multistep synthesis using raw materials derived from nonrenewable petrochemicals. Recently, the usage of naturally occurring organic linkers such as saccharides, amino acids, and nucleotides has attracted much attention for synthesis of a new class of MOFs called “Bio-MOFs”.⁶⁶ Implementation of Bio-MOFs either as pristine materials or as composites can potentially allow a green, sustainable, and eco-friendly approach for oil/water separation. In this section, some recent examples of Bio-MOFs and their composites used in oil/water separation are discussed. Mohamed et al. reported recently a copper-based Bio-MOF, Cu-Asp-MOF, using aspartic acid as a linker prepared by an electrochemical method.³³ The authors used stearic acid as a surfactant to reduce the surface energy of Cu-Asp-MOF. Fiber textile was then chosen as the supporting surface to fabricate a “biodegradable” MOF composite. The pristine textile showed a very smooth surface (Figure 15) with WCA = 0° , in contrast to the Cu-Asp-MOF-deposited superhydrophobic textile fiber composite, TF@Cu-Asp-MOF, with WCA = $158^\circ \pm 1^\circ$. The absorption capacities of the TF@Cu-Asp-MOF composite for *n*-hexane, petroleum ether, and silicon oil were reported as 85, 110, and 160 wt %, respectively,

for 10 cycles, with a separation efficiency ranging between 95.0% and 99.4%.

More recently Li and co-workers reported the synthesis of carbon nitride–copper MOF-based composite (CN-Cu-MOF) with a WCA of $150^\circ \pm 2^\circ$, indicating the superhydrophobic nature of this MOF.⁶⁵ In order to develop an environmentally benign composite, the group used a simple soaking method to deposit C_3N_4 -Cu-MOF on a cotton surface. The resulting CN/Cu-MOF@cotton showed a separation efficiency of 99% for up to 10 cycles, with excellent stability in highly acidic and alkaline conditions and high adsorption capacity for different oil/water mixtures, namely, castor oil, engine oil, and canola oil, without any noticeable degradation in efficiency.

Due to its appealing biodegradability, cellulose recently has been incorporated into composites with hydrophobic MOF materials for applications in oil/water separation. For example, ZIF-8 has been used to develop a cellulose acetate foam composite, ZIF-8@CA, via a thermally induced nonsolvent-induced phase separation method.³⁸ This composite showed a highly hydrophobic nature, as indicated by relatively high WCA (153°) and moderate adsorption capacity range of 6.89–14.61 wt % for *n*-hexane, xylene, and soybean oil/water mixtures, and a separation efficiency of 98.7% for up to six cycles. In another study, Lu et al. fabricated cellulose fiber composites of MIL-100(Fe) with catalytic activity. The cellulose fibers were first carboxymethylated with ($-\text{COOH}$) groups, followed by the deposition of MIL-100(Fe) on the cotton fiber surface via in situ growth.⁷⁸ Following this, AgCl crystals were formed on the MOF composite via the layer-by-

layer method. Ag nanoparticles were formed in situ on the surface of the composite to result in a Ag@AgCl@MIL-100(Fe)/CCF composite, which exhibited hydrophilic activity and underwater oleophilicity.

6. CURRENT CHALLENGES AND FUTURE DIRECTION

Despite the great promise of MOFs and their composites in oil/water separation, these materials should have good hydrolytic stability under both acidic and alkaline conditions for their practical applications. Although some recently developed MOFs have shown enhanced hydrolytic stability, the majority of MOFs are prone to rapid degradation in water. It must be noted that the interfacial interaction between MOFs and the supporting matrix (such as polymer, graphene oxide, etc.) plays a very important role in the stability of the resulting composites and, therefore, should be studied in detail. For example, a reverse approach for developing a hydrophilic MOF–polymer composite has been studied recently.⁷⁷ Other great challenges associated with water/oil separation are linked to the type of separation materials (adsorbent or membrane) used, namely, transferring and processing of the bulk material after each separation cycle,⁸⁵ recyclability, scalability, and cost. When considering materials for large-scale oil/water separation, factors related to recyclability and sustainability are of great concern. Currently, the development of recyclable MOFs, Bio-MOFs, and biodegradable MOFs has attracted much attention and is being considered as the future direction of MOF-based materials for oil/water separation.⁸⁶ Implementation of MOFs in bulk water treatment is still unexplored, and for large-scale applications MOFs need to be manufactured from cost-effective as well as renewable feedstocks and resources. Being a relatively new area, the cost of the scalable MOF composites has yet to be explored. Sustainability and recyclability are going to be more crucial for future applications, and the lifecycle assessment and circularity of the materials will need to be studied in more detail for practical implementation.⁸⁷ Being a relatively new area, there is also a lack of consistency in reporting the efficiency of the materials. For example, permeation data provides a better way to compare effectiveness compared to flux, and more coherence in the reported results will help to address this issue.³⁶ The emerging trend of using machine learning to identify promising MOFs (as being applied in other areas, such as hydrogen storage) is also expected to contribute to the development of more efficient MOF–polymer composites for oil/water separation.^{88,89}

7. CONCLUSION

Purification of water contaminated with oil can aid in the remediation of water and can help to prevent ecological damage from oil spills and urban and industrial pollution. Recently, various materials and methods have been studied for this important application due to their intriguing properties, including ultrahigh surface areas, tunable pore geometries and chemical properties, and surface adaptability, with numerous studies exploring the development of hydrophobic MOFs for selective adsorption of the oil phase. In this Review, the recent developments and main strategies of using MOFs and their composites in oil/water separation have been discussed. Common approaches involve the use of aromatic, fluorine, or long-chain alkyl-functionalized linkers as building blocks for the synthesis of hydrophobic MOFs. The symmetry of the

linker, as well as its coordination with the metal clusters, also contributes to surface morphologies and surface energies that may induce hydrophobicity. Other strategies involve the post-synthetic modification of the MOFs by the addition of hydrophobic functional groups containing fluorine and long-chain alkyl groups either on the linker or as capping ligands on the coordinatively unsaturated metal ions. Additionally, the recent focus on composites has shown that the MOFs can be incorporated into a composite material for the enhancement of certain features like stability, hydrophobicity, and processability and may also provide a synergistic effect on the enhancement of hydrophobicity. Several materials for the fabrication of composites have been used, including graphene oxide, metal meshes, and melamine sponges. More recently, biodegradable polymers, such as cellulose and polylactic acid, have been investigated for more environmentally friendly MOF–polymer composites for oil/water separation. With the rising number of studies, the importance of this class of materials is evident, and it can be assumed that the current concern over environmental pollution caused by direct and indirect oil spillage deserves more material-based approaches to find solutions for this critical problem, which is directly linked to “access of clean water” and “life below water”, two of the Sustainable Development Goals (SDGs) set by the United Nations.

AUTHOR INFORMATION

Corresponding Author

Sanjit Nayak – Bristol Composite Institute, School of Civil Aerospace and Design Engineering, University of Bristol, Bristol BS8 1TR, United Kingdom; orcid.org/0000-0002-0342-9860; Email: s.nayak@bristol.ac.uk

Authors

Abdullah M. Abudayyeh – Institute of Condensed Matter and Nanosciences (IMCN), Université catholique de Louvain, Louvain-la-Neuve, Walloon Brabant BE 1348, Belgium

Lila A.M. Mahmoud – School of Chemistry, University of Bristol, Bristol BS8 1TS, United Kingdom; orcid.org/0000-0003-3625-0602

Valeska P. Ting – Research School of Chemistry & College of Engineering, Computing and Cybernetics, The Australian National University, Canberra ACT 2602, Australia; orcid.org/0000-0003-3049-0939

Complete contact information is available at: <https://pubs.acs.org/10.1021/acsomega.4c07911>

Author Contributions

[▽]AMA and LAMM contributed equally.

Notes

The authors declare no competing financial interest.

ACKNOWLEDGMENTS

AMA and LAMM acknowledge support from the Erasmus+ Exchange programme. VPT and SN acknowledge support from the Engineering and Physical Sciences Research Council (EP/R01650X/1 and EP/S021728/1).

REFERENCES

(1) Guerin, T. F. Heavy equipment maintenance wastes and environmental management in the mining industry. *J. Environ. Manag.* 2002, 66, 185–199.

- (2) U.S. EPA *Hydraulic Fracturing for Oil and Gas: Impacts from the Hydraulic Fracturing Water Cycle on Drinking Water Resources in the United States (Final Report)*; EPA/600/R-16/236F; U.S. Environmental Protection Agency: Washington, DC, 2016.
- (3) Dubansky, B.; Whitehead, A.; Miller, J. T.; Rice, C. D.; Galvez, F. Multitissue Molecular, Genomic, and Developmental Effects of the Deepwater Horizon Oil Spill on Resident Gulf Killifish (*Fundulus grandis*). *Environ. Sci. Technol.* **2013**, *47*, 5074–5082.
- (4) Aguilera, F.; Méndez, J.; Pásaro, E.; Laffon, B. Review on the effects of exposure to spilled oils on human health. *J. Appl. Toxicol.* **2010**, *30*, 291–301.
- (5) Shannon, M. A.; Bohn, P. W.; Elimelech, M.; Georgiadis, J. G.; Mariñas, B. J.; Mayes, A. M. Science and technology for water purification in the coming decades. *Nature* **2008**, *452*, 301–310.
- (6) Rojas, S.; Horcajada, P. Metal–Organic Frameworks for the Removal of Emerging Organic Contaminants in Water. *Chem. Rev.* **2020**, *120*, 8378–8415.
- (7) Jiang, Y.-H.; Zhang, Y.-Q.; Wang, Z.-H.; An, Q.-D.; Xiao, Z.-Y.; Xiao, L.-P.; Zhai, S.-R. Cotton-derived green sustainable membrane with tailored wettability interface: Synergy of lignin and ethyl cellulose. *Ind. Crop. Prod.* **2022**, *183*, No. 114993.
- (8) Jiang, Y.-H.; Zhang, Y.-Q.; Wang, Z.-H.; An, Q.-D.; Xiao, Z.-Y.; Xiao, L.-P.; Zhai, S.-R. Controllable construction of multifunctional superhydrophobic coating with ultra-stable efficiency for oily water treatment. *J. Colloid Interface Sci.* **2022**, *628*, 356–365.
- (9) Wang, B.; Liang, W.; Guo, Z.; Liu, W. Biomimetic superhydrophobic and superhydrophilic materials applied for oil/water separation: a new strategy beyond nature. *Chem. Soc. Rev.* **2015**, *44*, 336–361.
- (10) Lee, C. H.; Tiwari, B.; Zhang, D.; Yap, Y. K. Water purification: oil–water separation by nanotechnology and environmental concerns. *Environ. Sci.: Nano* **2017**, *4*, 514–525.
- (11) Mir, S.; Naderifar, A.; Rahidi, A. m.; Alaei, M. Recent advances in oil/water separation using nanomaterial-based filtration methods for crude oil processing—a review. *J. Petrol. Sci. Eng.* **2022**, *215*, No. 110617.
- (12) Gore, P. M.; Purushothaman, A.; Naebe, M.; Wang, X.; Kandasubramanian, B., *Nanotechnology for Oil-Water Separation*. In *Advanced Research in Nanosciences for Water Technology*; Prasad, R., Karchiyappan, T., Eds.; Springer International Publishing, 2019; pp 299–339.
- (13) Rego, R. M.; Kuriya, G.; Kurkuri, M. D.; Kigga, M. MOF based engineered materials in water remediation: Recent trends. *J. Hazard. Mater.* **2021**, *403*, No. 123605.
- (14) Liu, K.; Cao, M.; Fujishima, A.; Jiang, L. Bio-Inspired Titanium Dioxide Materials with Special Wettability and Their Applications. *Chem. Rev.* **2014**, *114*, 10044–10094.
- (15) Kwon, G.; Kota, A. K.; Li, Y.; Sohani, A.; Mabry, J. M.; Tuteja, A. On-Demand Separation of Oil-Water Mixtures. *Adv. Mater.* **2012**, *24*, 3666–3671.
- (16) Yaghi, O. M.; O’Keeffe, M.; Ockwig, N. W.; Chae, H. K.; Eddaoudi, M.; Kim, J. Reticular synthesis and the design of new materials. *Nature* **2003**, *423*, 705–714.
- (17) Li, J.-R.; Kuppler, R. J.; Zhou, H.-C. Selective gas adsorption and separation in metal–organic frameworks. *Chem. Soc. Rev.* **2009**, *38*, 1477–1504.
- (18) Ma, S.; Zhou, H.-C. Gas storage in porous metal–organic frameworks for clean energy applications. *Chem. Commun.* **2010**, *46*, 44–53.
- (19) Na, K.; Choi, K. M.; Yaghi, O. M.; Somorjai, G. A. Metal Nanocrystals Embedded in Single Nanocrystals of MOFs Give Unusual Selectivity as Heterogeneous Catalysts. *Nano Lett.* **2014**, *14*, 5979–5983.
- (20) Yuan, H.; Li, N.; Fan, W.; Cai, H.; Zhao, D. Metal–Organic Framework Based Gas Sensors. *Adv. Sci.* **2022**, *9*, No. 2104374.
- (21) Kobielska, P. A.; Howarth, A. J.; Farha, O. K.; Nayak, S. Metal–organic frameworks for heavy metal removal from water. *Coord. Chem. Rev.* **2018**, *358*, 92–107.
- (22) Mahmoud, L. A. M.; Telford, R.; Livesey, T. C.; Katsikogianni, M.; Kelly, A. L.; Terry, L. R.; Ting, V. P.; Nayak, S. Zirconium-Based MOFs and Their Biodegradable Polymer Composites for Controlled and Sustainable Delivery of Herbicides. *ACS Appl. Bio Mater.* **2022**, *5*, 3972–3981.
- (23) Reis, R. A. d.; Mahmoud, L. A. M.; Ivanovska, E. H.; Telford, R.; Addicoat, M. A.; Terry, L. R.; Ting, V. P.; Nayak, S. Biodegradable Polymer–Metal–Organic Framework (MOF) Composites for Controlled and Sustainable Pesticide Delivery. *Adv. Sustain. Syst.* **2023**, *7*, No. 2300269.
- (24) Horcajada, P.; Chalati, T.; Serre, C.; Gillet, B.; Sebrie, C.; Baati, T.; Eubank, J. F.; Heurtaux, D.; Clayette, P.; Kreuz, C.; Chang, J.-S.; Hwang, Y. K.; Marsaud, V.; Bories, P.-N.; Cynober, L.; Gil, S.; Férey, G.; Couvreur, P.; Gref, R. Porous metal–organic-framework nanoscale carriers as a potential platform for drug delivery and imaging. *Nat. Mater.* **2010**, *9*, 172–178.
- (25) Aden, S. F.; Mahmoud, L. A.; Ivanovska, E. H.; Terry, L. R.; Ting, V. P.; Katsikogianni, M. G.; Nayak, S. Controlled Delivery of Ciprofloxacin Using Zirconium-Based MOFs and Poly-Caprolactone Composites. *J. Drug Delivery Sci. Technol.* **2023**, *88*, No. 104894.
- (26) Livesey, T. C.; Mahmoud, L. A. M.; Katsikogianni, M. G.; Nayak, S. Metal–Organic Frameworks and Their Biodegradable Composites for Controlled Delivery of Antimicrobial Drugs. *Pharmaceutics* **2023**, *15*, 274.
- (27) Jayaramulu, K.; Geyer, F.; Schneemann, A.; Kment, Š.; Otyepka, M.; Zboril, R.; Vollmer, D.; Fischer, R. A. Hydrophobic Metal–Organic Frameworks. *Adv. Mater.* **2019**, *31*, No. 1900820.
- (28) Russo, V.; Hmoudah, M.; Broccoli, F.; Iesce, M. R.; Jung, O.-S.; Di Serio, M. Applications of Metal Organic Frameworks in Wastewater Treatment: A Review on Adsorption and Photodegradation. *Front. Chem. Eng.* **2020**, *2*, 581487.
- (29) Xie, L.-H.; Xu, M.-M.; Liu, X.-M.; Zhao, M.-J.; Li, J.-R. Hydrophobic Metal–Organic Frameworks: Assessment, Construction, and Diverse Applications. *Adv. Sci.* **2020**, *7*, No. 1901758.
- (30) Jayaramulu, K.; Datta, K. K. R.; Rösler, C.; Petr, M.; Otyepka, M.; Zboril, R.; Fischer, R. A. Biomimetic Superhydrophobic/Superoleophilic Highly Fluorinated Graphene Oxide and ZIF-8 Composites for Oil–Water Separation. *Angew. Chem., Int. Ed.* **2016**, *55*, 1178–1182.
- (31) Kalaj, M.; Bentz, K. C.; Ayala, S., Jr.; Palomba, J. M.; Barcus, K. S.; Katayama, Y.; Cohen, S. M. MOF-Polymer Hybrid Materials: From Simple Composites to Tailored Architectures. *Chem. Rev.* **2020**, *120*, 8267–8302.
- (32) Shi, M.; Huang, R.; Qi, W.; Su, R.; He, Z. Synthesis of superhydrophobic and high stable Zr-MOFs for oil-water separation. *Colloids Surf. A: Physicochem. Eng.* **2020**, *602*, No. 125102.
- (33) Mohamed, M. E.; Abd-El-Nabey, B. A. Fabrication of a biological metal–organic framework based superhydrophobic textile fabric for efficient oil/water separation. *Sci. Rep.* **2022**, *12*, 15483.
- (34) Zin, G.; Wu, J.; Rezzadori, K.; Petrus, J. C. C.; Di Luccio, M.; Li, Q. Modification of hydrophobic commercial PVDF microfiltration membranes into superhydrophilic membranes by the mussel-inspired method with dopamine and polyethyleneimine. *Sep. Purif. Technol.* **2019**, *212*, 641–649.
- (35) He, M.; Wang, P.; Zhang, R.; Jiang, Z.; He, X.; Ma, J. Oil/water separation membranes with a fluorine island structure for stable high flux. *J. Mater. Chem. A* **2021**, *9* (11), 6905–6912.
- (36) Ni, T.; Kong, L.; Xie, Z.; Lin, J.; Zhao, S. Flux vs. permeability: How to effectively evaluate mass transfer performance of membranes in oil-water separation. *J. Water Process. Eng.* **2022**, *49*, No. 103119.
- (37) Krahnstöver, T.; Hochstrat, R.; Wintgens, T. Comparison of methods to assess the integrity and separation efficiency of ultrafiltration membranes in wastewater reclamation processes. *J. Water Process. Eng.* **2019**, *30*, No. 100646.
- (38) Wang, S.; Gao, Z.; Qi, X.; Li, C.; Xie, Y.; Yang, X.; Song, W.; Liu, Z. Eco-friendly superhydrophobic MOF-doped with cellulose acetate foam for efficient oil-water separation. *J. Environ. Chem. Eng.* **2022**, *10*, No. 108521.

- (39) Rana, A.; Ghosh, S.; Biswas, S. An eco-friendly approach using a nonfluorous self-cleaning metal–organic framework composite and membrane for oil–water separation. *Inorg. Chem. Front.* **2023**, *10*, 612–620.
- (40) Crane, A. K.; White, N. G.; MacLachlan, M. J. Metal organic frameworks from extended, conjugated pentiptycene-based ligands. *CrystEngComm* **2015**, *17*, 4912–4918.
- (41) Zhang, M.; Xin, X.; Xiao, Z.; Wang, R.; Zhang, L.; Sun, D. A multi-aromatic hydrocarbon unit induced hydrophobic metal–organic framework for efficient C2/C1 hydrocarbon and oil/water separation. *J. Mater. Chem. A* **2017**, *5*, 1168–1175.
- (42) Zhang, M.; Guo, B.; Feng, Y.; Xie, C.; Han, X.; Kong, X.; Xu, B.; Zhang, L. Amphipathic Pentiptycene-Based Water-Resistant Cu-MOF for Efficient Oil/Water Separation. *Inorg. Chem.* **2019**, *58*, 5384–5387.
- (43) Chen, Y.; Wang, B.; Wang, X.; Xie, L.-H.; Li, J.; Xie, Y.; Li, J.-R. A Copper(II)-Paddlewheel Metal–Organic Framework with Exceptional Hydrolytic Stability and Selective Adsorption and Detection Ability of Aniline in Water. *ACS Appl. Mater. Interfaces* **2017**, *9*, 27027–27035.
- (44) Chong, J. H.; MacLachlan, M. J. Iptycenes in supramolecular and materials chemistry. *Chem. Soc. Rev.* **2009**, *38*, 3301–3315.
- (45) Zhu, X.-Z.; Chen, C.-F. A Highly Efficient Approach to [4]Pseudocatenanes by Threefold Metathesis Reactions of a Triptycene-Based Tris[2]pseudorotaxane. *J. Am. Chem. Soc.* **2005**, *127*, 13158–13159.
- (46) Zhang, M.; Zhang, L.; Xiao, Z.; Zhang, Q.; Wang, R.; Dai, F.; Sun, D. Pentiptycene-Based Luminescent Cu (II) MOF Exhibiting Selective Gas Adsorption and Unprecedentedly High-Sensitivity Detection of Nitroaromatic Compounds (NACs). *Sci. Rep.* **2016**, *6*, 20672.
- (47) Roy, S.; Suresh, V. M.; Maji, T. K. Self-cleaning MOF: realization of extreme water repellence in coordination driven self-assembled nanostructures. *Chem. Sci.* **2016**, *7*, 2251–2256.
- (48) Yang, C.; Kaipa, U.; Mather, Q. Z.; Wang, X.; Nesterov, V.; Venero, A. F.; Omary, M. A. Fluorous Metal–Organic Frameworks with Superior Adsorption and Hydrophobic Properties toward Oil Spill Cleanup and Hydrocarbon Storage. *J. Am. Chem. Soc.* **2011**, *133*, 18094–18097.
- (49) Chen, T.-H.; Popov, I.; Zenasni, O.; Daugulis, O.; Miljanić, O. Š. Superhydrophobic perfluorinated metal–organic frameworks. *Chem. Commun.* **2013**, *49*, 6846–6848.
- (50) Gogoi, C.; Rana, A.; Ghosh, S.; Fopase, R.; Pandey, L. M.; Biswas, S. Superhydrophobic Self-Cleaning Composite of a Metal–Organic Framework with Polypropylene Fabric for Efficient Removal of Oils from Oil–Water Mixtures and Emulsions. *ACS Appl. Nano Mater.* **2022**, *5*, 10003–10014.
- (51) Sun, T.; Hao, S.; Fan, R.; Qin, M.; Chen, W.; Wang, P.; Yang, Y. Hydrophobicity-Adjustable MOF Constructs Superhydrophobic MOF-rGO Aerogel for Efficient Oil–Water Separation. *ACS Appl. Mater. Interfaces* **2020**, *12*, 56435–56444.
- (52) Mukherjee, S.; Kansara, A. M.; Saha, D.; Gonnade, R.; Mullangi, D.; Manna, B.; Desai, A. V.; Thorat, S. H.; Singh, P. S.; Mukherjee, A.; Ghosh, S. K. An Ultrahydrophobic Fluorous Metal–Organic Framework Derived Recyclable Composite as a Promising Platform to Tackle Marine Oil Spills. *Chem.-Eur. J.* **2016**, *22*, 10937–10943.
- (53) He, L.; Guo, Y. J.; Xiao, Y. H.; Chen, E. X.; Luo, M. B.; Li, Z. H.; Lin, Q. P. Imparting Superhydrophobicity to Porphyrinic Coordination Frameworks Using Organotin. *CCS Chem.* **2022**, *4*, 2286–2293.
- (54) Rao, K. P.; Higuchi, M.; Sumida, K.; Furukawa, S.; Duan, J.; Kitagawa, S. Design of Superhydrophobic Porous Coordination Polymers through the Introduction of External Surface Corrugation by the Use of an Aromatic Hydrocarbon Building Unit. *Angew. Chem., Int. Ed.* **2014**, *53*, 8225–8230.
- (55) Rodríguez-Hermida, S.; Tsang, M. Y.; Vignatti, C.; Stylianou, K. C.; Guillerm, V.; Pérez-Carvajal, J.; Teixidor, F.; Viñas, C.; Choquesillo-Lazarte, D.; Verdugo-Escamilla, C.; Peral, I.; Juanhuix, J.; Verdager, A.; Imaz, I.; Maspocho, D.; Giner Planas, J. Switchable Surface Hydrophobicity–Hydrophilicity of a Metal–Organic Framework. *Angew. Chem., Int. Ed.* **2016**, *55*, 16049–16053.
- (56) Pournara, A. D.; Rizogianni, S.; Evangelou, D. A.; Andreou, E. K.; Armatas, G. S.; Manos, M. J. Zr⁴⁺-terephthalate MOFs with 6-connected structures, highly efficient As(III/V) sorption and superhydrophobic properties. *Chem. Commun.* **2022**, *58*, 8862–8865.
- (57) Venturi, D. M.; Costantino, F. Recent advances in the chemistry and applications of fluorinated metal-organic frameworks (F-MOFs). *RSC Adv.* **2023**, *13*, 29215–29230.
- (58) Yang, C.; Wang, X.; Omary, M. A. Fluorous Metal–Organic Frameworks for High-Density Gas Adsorption. *J. Am. Chem. Soc.* **2007**, *129*, 15454–15455.
- (59) Chen, T.; Zhao, D. Post-synthetic modification of metal-organic framework-based membranes for enhanced molecular separations. *Coord. Chem. Rev.* **2023**, *491*, No. 215259.
- (60) Sun, D.; Adiyala, P. R.; Yim, S. J.; Kim, D. P. Pore-Surface Engineering by Decorating Metal-Oxo Nodes with Phenylsilane to Give Versatile Super-Hydrophobic Metal-Organic Frameworks (MOFs). *Angew. Chem.-Int. Ed.* **2019**, *58*, 7405–7409.
- (61) Gao, M.-L.; Zhao, S.-Y.; Chen, Z.-Y.; Liu, L.; Han, Z.-B. Superhydrophobic/Superoleophilic MOF Composites for Oil–Water Separation. *Inorg. Chem.* **2019**, *58*, 2261–2264.
- (62) Nguyen, J. G.; Cohen, S. M. Moisture-Resistant and Superhydrophobic Metal–Organic Frameworks Obtained via Post-synthetic Modification. *J. Am. Chem. Soc.* **2010**, *132*, 4560–4561.
- (63) Li, H.; Zhu, L.; Zhu, X.; Chao, M.; Xue, J.; Sun, D.; Xia, F.; Xue, Q. Dual-functional membrane decorated with flower-like metal–organic frameworks for highly efficient removal of insoluble emulsified oils and soluble dyes. *J. Hazard. Mater.* **2021**, *408*, No. 124444.
- (64) Liu, C.; Liu, Q.; Huang, A. A superhydrophobic zeolitic imidazolate framework (ZIF-90) with high steam stability for efficient recovery of bioalcohols. *Chem. Commun.* **2016**, *52*, 3400–3402.
- (65) Wang, H.; Meng, J.; Li, F.; Li, T. Graphitic carbon nitride/metal-organic framework composite functionalized cotton for efficient oil-water separation and dye degradation. *J. Clean. Prod.* **2023**, *385*, No. 135758.
- (66) Nadar, S. S.; Vaidya, L.; Maurya, S.; Rathod, V. K. Polysaccharide based metal organic frameworks (polysaccharide–MOF): A review. *Coord. Chem. Rev.* **2019**, *396*, 1–21.
- (67) González, C. M. O.; Tellez, A. d. M. N.; Kharisov, B. I.; Kharisova, O. V.; Quezada, T. E. S.; González, L. T. Hydrophobic mixed-metal MOF-derived carbon sponges. *Mendeleev Commun.* **2021**, *31*, 91–93.
- (68) Ghosh, S.; Rana, A.; Kumar, S.; Gogoi, C.; Mukherjee, S.; Manna, U.; Biswas, S. A self-cleaning hydrophobic MOF-based composite for highly efficient and recyclable separation of oil from water and emulsions. *Mater. Chem. Front.* **2022**, *6*, 2051–2060.
- (69) Li, Y.; Lin, Z.; Wang, X.; Duan, Z.; Lu, P.; Li, S.; Ji, D.; Wang, Z.; Li, G.; Yu, D.; Liu, W. High-hydrophobic ZIF-8@PLA composite aerogel and application for oil-water separation. *Sep. Purif. Technol.* **2021**, *270*, No. 118794.
- (70) Qu, W.; Wang, Z.; Wang, X.; Wang, Z.; Yu, D.; Ji, D. High-hydrophobic ZIF-67@PLA honeycomb aerogel for efficient oil–water separation. *Colloids Surf. A: Physicochem. Eng.* **2023**, *658*, No. 130768.
- (71) Zhang, L.; Xie, J.; Luo, X.; Gong, X.; Zhu, M. Enhanced hydrophobicity of shell-ligand-exchanged ZIF-8/melamine foam for excellent oil-water separation. *Chem. Eng. Sci.* **2023**, *273*, No. 118663.
- (72) Bauza, M.; Turnes Palomino, G.; Palomino Cabello, C. MIL-100(Fe)-derived carbon sponge as high-performance material for oil/water separation. *Sep. Purif. Technol.* **2021**, *257*, No. 117951.
- (73) Zhang, L.; Wei, L. X.; Jia, X. L.; Geng, X. H.; Liu, C. Preparation and characterization of nano-demulsifier ZIF-8@CNTs based on MOFs for O/W emulsion demulsification. *J. Dispersion Sci. Technol.* **2023**, *44*, 2393–2402.
- (74) Han, X. Y.; Ma, W. X.; Zhang, H. R.; Chen, G. E.; Shi, Y.; Xu, Z. L. Self assembled PP membrane with photocatalytic self-cleaning performance for efficient oil/water emulsion separation. *Colloid Surf. A-Physicochem. Eng. Asp.* **2023**, *669*, 131383.

(75) Obaid, M.; Alsadun, N.; Shekhah, O.; Almahfoodh, S.; Zhou, S.; Ghaffour, N.; Eddaoudi, M. Deployment of Superhydrophilic and Super-antifouling Cr-soc-MOF-1-Based Membrane for Ultrafast Separation of Stabilized Oil-in-Water Emulsions. *ACS Appl. Mater. Interfaces* **2023**, *15*, 31067–31076.

(76) He, H. Q.; Liu, Y. J.; Zhu, Y. M.; Zhang, T. C.; Yuan, S. J. Underoil superhydrophilic Cu₂O₄@Cu-MOFs core-shell nano-sheets-coated copper mesh membrane for on-demand emulsion separation and simultaneous removal of soluble dye. *Sep. Purif. Technol.* **2022**, *293*, No. 121089.

(77) Ye, Q.; Xu, J.-M.; Zhang, Y.-J.; Chen, S.-H.; Zhan, X.-Q.; Ni, W.; Tsai, L.-C.; Jiang, T.; Ma, N.; Tsai, F.-C. Metal-organic framework modified hydrophilic polyvinylidene fluoride porous membrane for efficient degerming selective oil/water emulsion separation. *npj Clean Water* **2022**, *5*, 23.

(78) Lu, W.; Duan, C.; Liu, C.; Zhang, Y.; Meng, X.; Dai, L.; Wang, W.; Yu, H.; Ni, Y. A self-cleaning and photocatalytic cellulose-fiber-supported "Ag@AgCl@MOF- cloth" membrane for complex wastewater remediation. *Carbohydr. Polym.* **2020**, *247*, No. 116691.

(79) Yuan, N.; Gong, X. R.; Han, B. H. Hydrophobic Fluorous Metal-Organic Framework Nanoadsorbent for Removal of Hazardous Wastes from Water. *ACS Appl. Nano Mater.* **2021**, *4*, 1576–1585.

(80) Deng, J. H.; Wen, Y. Q.; Willman, J.; Liu, W. J.; Gong, Y. N.; Zhong, D. C.; Lu, T. B.; Zhou, H. C. Facile Exfoliation of 3D Pillared Metal-Organic Frameworks (MOFs) to Produce MOF Nanosheets with Functionalized Surfaces. *Inorg.Chem.* **2019**, *58*, 11020–11027.

(81) Ata-ur-Rehman; Tirmizi, S. A.; Badshah, A.; Ammad, H. M.; Jawad, M.; Abbas, S. M.; Rana, U. A.; Khan, S. U.-D. Synthesis of highly stable MOF-5@MWCNTs nanocomposite with improved hydrophobic properties. *Arab. J. Chem.* **2018**, *11*, 26–33.

(82) Xiang, W. L.; Gong, S. Y.; Zhu, J. B. Eco-Friendly Fluorine Functionalized Superhydrophobic/Superoleophilic Zeolitic Imidazolate Frameworks-Based Composite for Continuous Oil-Water Separation. *Molecules* **2023**, *28*, 2843.

(83) Song, M.; Zhao, Y.; Mu, S.; Jiang, C.; Li, Z.; Yang, P.; Fang, Q.; Xue, M.; Qiu, S. A stable ZIF-8-coated mesh membrane with micro-/nano architectures produced by a facile fabrication method for high-efficiency oil-water separation. *Sci. China Mater.* **2019**, *62*, 536–544.

(84) Zhou, Y.; Wang, Y.; Chen, Z.; Gong, H.; Chen, L.; Yu, H. Highly Hydrophilic ZIF-8 as a Carbonic Anhydrase Mimetic Catalyst for Promoting CO₂ Absorption. *J. Phys. Chem. C* **2023**, *127*, 7184–7196.

(85) Montewka, J.; Weckström, M.; Kujala, P. A probabilistic model estimating oil spill clean-up costs – A case study for the Gulf of Finland. *Mar. Pollut. Bull.* **2013**, *76*, 61–71.

(86) Hashemi, L.; Masoomi, M. Y.; Garcia, H. Regeneration and reconstruction of metal-organic frameworks: Opportunities for industrial usage. *Coord. Chem. Rev.* **2022**, *472*, No. 214776.

(87) Grande, C. A.; Blom, R.; Spjelkavik, A.; Moreau, V.; Payet, J. Life-cycle assessment as a tool for eco-design of metal-organic frameworks (MOFs). *Sustain. Mater. Technol.* **2017**, *14*, 11–18.

(88) Yuan, X.; Deng, X.; Cai, C.; Shi, Z.; Liang, H.; Li, S.; Qiao, Z. Machine learning and high-throughput computational screening of hydrophobic metal-organic frameworks for capture of formaldehyde from air. *Green Energy Environ.* **2021**, *6*, 759–770.

(89) Ahmed, A.; Siegel, D. J. Predicting hydrogen storage in MOFs via machine learning. *Patterns* **2021**, *2*, No. 100291.